Refinement of tracer dilution methods for discharge measurements in steep mountain streams

by

Mark E. Richardson

B.Sc., Civil and Environmental Engineering, Case Western Reserve University, U.S.A, 2012

B.A., Computer Science, Case Western Reserve University, U.S.A., 2012

A THESIS SUBMITTED IN PARTIAL FULFILLMENT
OF THE REQUIREMENTS FOR THE DEGREE OF

Master of Science

in

THE FACULTY OF GRADUATE AND POSTDOCTORAL STUDIES

(Geography)

The University of British Columbia

(Vancouver)

September 2015

© Mark E. Richardson, 2015

Abstract

Tracer dilution methods using salt and Rhodamine WT (RWT) are commonly used to measure discharge in steep mountain streams. This research addressed knowledge gaps associated with dilution methods using original field data collected on nine streams in southwest British Columbia and discharge measurements conducted by Northwest Hydraulic Consultants. Laboratory experiments were conducted to evaluate the uncertainties associated with different procedures for calibrating the relation between salt concentration and electrical conductivity (*EC*) for dry salt injection, and to evaluate the effects of RWT decay due to sorption and photolysis.

For salt dilution, calibration should be conducted at the in-situ stream temperature for greatest accuracy. The calibration factor varied linearly with background *EC* for water samples with *EC* less than 1000 µS/cm. For higher background *EC*, factors plotted below the fitted relation, likely due to differences in the relative ionic abundances.

Minimum mixing lengths ranged between 6.5 and 24.5 stream wetted widths, but determining the mixing length can be confounded by surface-subsurface water fluxes. Probes need to be placed on opposite sides of the stream to verify adequate mixing, because probes located at different locations on the same of the stream sometimes suggested complete mixing had occurred when it in fact had not. For probes located downstream of complete mixing, breakthrough curves (BTCs) for probes located in the main current differed significantly from probes in zones with recirculating flow, even though they yielded discharge values within $\pm$ 10%.

The peak of the BTC is a function of the mass of tracer injected, reach length, channel cross-sectional area, and the integral of a non-dimensional BTC, A^*. The distribution of A^* derived from analysis of 175 BTCs can be used, in conjunction with estimates of channel geometry and desired increases in *EC*, to estimate dosing requirements to avoid under- or over-dosing a stream reach.

The calibration factor for RWT varied with turbidity, indicating that calibration is essential for each discharge measurement. Laboratory and field experiments focused on RWT decay were confounded by other factors, so no firm conclusions could be drawn.

Preface

This thesis is original work completed by the author. Guidance was given by the supervisory committee: Dan Moore, Brett Eaton, and André Zimmermann.

A version of work in sections 3.1, 3.3, and 3.5.1 has been presented as a poster: "Advancements in tracer dilution gauging: quantifying uncertainties in streamflow data" (Richardson, M., Moore, R.D. and Zimmermann, A.). The author acted as lead investigator and presented the poster at the AGU-GAC-MAC-CGU Joint Assembly meeting on May 4, 2015, in Montreal, Quebec and at the Canadian Water Resources Association (CWRA) meeting on June 3, 2015, in Winnipeg, Manitoba.

A version of the results in section 3.1 has been presented with the title "Derivation, uncertainty, and variance of the calibration factor used in salt dilution flow measurements" (Sentlinger, G., Zimmermann, A., Richardson, M. and Fraser, J.). The author provided data and analysis results for the presentation material. The presentation was given at the American Water Association (AWRA) meeting on November 4, 2014, in Tysons Corner, U.S.A., and at the International Conference on Forests and Water in a Changing Environment (IUFRO) meeting on July 7, 2015, in Kelowna, British Columbia.

Table of Contents

Abstract . . . . . **ii**

Preface . . . . . **iii**

Table of Contents . . . . . **iv**

List of Tables . . . . . **v**

List of Figures . . . . . **vi**

Acknowledgements . . . . . **vii**

1 Introduction **1**

1.1 Motivation for the study 1

1.2 Literature review 4

1.2.1 Salt dilution gauging 4

1.2.2 Rhodamine WT dye dilution gauging 8

1.3 Research objectives and thesis structure 9

2 Study sites and methodology **11**

2.1 Study sites 11

2.1.1 Field sites 11

2.1.2 Water sample sites 13

2.2 Field methods 14

2.2.1 Stream gauging for salt dilution 14

2.2.2 Measurement probe setup 17

2.2.3 Surveying 19

2.2.4 Stream gauging for Rhodamine WT dye dilution 19

2.3 Laboratory methods 20

2.3.1 Laboratory calibrations for salt dilution 20
2.3.2 Laboratory calibrations and laboratory experiment for Rhodamine WT dye dilution 23
2.4 Data analysis 24
2.4.1 Uncertainty analysis of discharge measurements 24
2.4.2 Mixing lengths 27
2.4.3 Relationships for dosing guidelines 27

3 Results 29
3.1 Calibration factors for salt dilution via dry slug injection 29
3.2 Mixing characteristics 33
3.3 Measurement location and discharge variability 33
3.4 Dosage guidelines: relations between $A*$ and reach characteristics 34
3.5 Rhodamine WT dilution gauging 43
3.5.1 Laboratory calibrations and experiment for Rhodamine WT 43
3.5.2 Stream gauging with Rhodamine WT 45

4 Discussion 48
4.1 Calibration factors for salt dilution via dry slug injection 48
4.1.1 Experiments 1 through 4 48
4.1.2 Experiment 5 - province-wide CF_T analysis 49
4.1.3 Guidelines for determining CF_T uncertainty 50
4.2 Mixing characteristics 51
4.3 Measurement location and discharge variability 54
4.4 Dosage guidelines 56
4.4.1 Relations between $A*$ and reach characteristics 56
4.4.2 Using A^* for dosage guidelines 58
4.5 Rhodamine WT dilution gauging 61
4.5.1 Laboratory calibrations and experiment for Rhodamine WT 61
4.5.2 Stream gauging with Rhodamine WT 62

5 Conclusions 65
5.1 Summary of key results 65
5.2 Future research 68

References 70

List of Tables

Table 1.1 Salt dilution dosage guidelines from various sources. 7

Table 2.1 Streams used in study 12
Table 2.2 Laboratory experiments for salt dilution calibration procedure 21
Table 2.3 Instruments and materials used for laboratory calibrations for salt dilution . . . 21
Table 2.4 Example calibration results using the distilled water correction used in this study 22

Table 3.1 Results from laboratory experiments for salt dilution calibration procedure . . . 29
Table 3.2 Statistical tests for laboratory experiments for salt dilution calibration procedure 30
Table 3.3 Cation and anion analyses results for selected water samples 31
Table 3.4 Multiple linear regression for CF_T vs. EC_{BG} for triple calibrations 32
Table 3.5 Mixing lengths determined from discharge measurements at multiple locations 34
Table 3.6 Discharge measurements for Carnation Creek Trib C 34
Table 3.7 Discharge measurements for injections focusing on measurement location variability 35
Table 3.8 Measurement location variability of A^* 39
Table 3.9 Results for each set (n = 7) of Rhodamine WT calibrations 43
Table 3.10 Statistical tests for comparisons between turbidity levels and between probes for Rhodamine WT calibrations 43
Table 3.11 CF_R values used for field discharge measurements 46
Table 3.12 Signal/noise observations for the RWT discharge measurements 46
Table 3.13 Discharge measurements for RWT and salt dilution gauging at Mosquito Creek, North Vancouver, BC 47

Table 4.1 Values of δ_{CF_T} for different calibration conditions, using an example CF_T value of 0.48 $\mathrm{L \cdot cm \cdot \mu S^{-1} \cdot m^{-3}}$ 51
Table 4.2 Values for determining A^* from example BTC in Figure 4.2 60
Table 4.3 Example salt dosage calculation using A^* 60

List of Figures

Figure 1.1 An example breakthrough curve (BTC) for a slug injection salt dilution discharge measurement. 3

Figure 2.1 Streams used in study 13
Figure 2.2 Field sites and water sample sites 15
Figure 2.3 Examples of experimental setups at Rutherford Creek and Pemberton Creek . . 18
Figure 2.4 Rhodamine WT laboratory experiment setup 24
Figure 2.5 Discharge measurement uncertainty breakdown for a a typical low uncertainty measurement and a typical high uncertainty measurement. 25

Figure 3.1 Relation between CF_T and background EC_T for salt dilution calibrations conducted in the laboratory and field 30
Figure 3.2 Relation between CF_T and background EC_T for salt dilution calibrations conducted with three probes concurrently 32
Figure 3.3 Stage-discharge relation for Bridge Glacier West Creek (data from Moyer, 2015) 35
Figure 3.4 BTCs for discharge measurements focused on measurement location variability 36
Figure 3.5 Plots of all non-dimensional BTCs 38
Figure 3.6 Boxplot of A^* values for all injections (field study streams and NHC streams) and for each field study stream. 39
Figure 3.7 Histograms of A^* values 40
Figure 3.8 Variability of A^* with discharge, for all injections from all field study streams (n = 121) 41
Figure 3.9 Variability of A^* with ratio of reach length to wetted width, for all injections from all field study streams (n = 121) 41
Figure 3.10 Variability of A^* with discharge, for a constant reach length, at Pemberton Creek 42
Figure 3.11 Variability of A^* with reach length, for constant discharge, at Carnation Creek Trib C 42

Figure 3.12 Time series plots of turbidity and Rhodamine WT for laboratory experiment . . 44
Figure 3.13 Rhodamine WT decay at different silt concentrations 45

Figure 4.1 Example BTC from Bridge Glacier South Creek 55
Figure 4.2 Example BTC transformation to determine A^* 59

Acknowledgements

This work is the result of efforts by many people. First, thanks go to my supervisor Dan Moore. Dan's enthusiam, ideas, and passion for this project were without bounds, and kept me focused and excited.The guidance and ideas from André Zimmermann during and after my internship at Northwest Hydraulic Consultants were invaluable to the success of this thesis. Thanks also go to Brett Eaton for showing me the streams of North Vancouver and for guidance in fluvial geomorphology. I learned an immense amount from my discussions with Frank van der Have, Dave Hutchinson, Robin Pike and Gabe Sentlinger.

Funding for this research project was provided by operating grants to Professor Dan Moore from Natural Sciences and Engineering Research Councel (NSERC) and by Northwest Hydraulic Consultants and Mitacs as part of a Mitacs Accelerate Internship.

Special thanks go to the many enthusiastic individuals who provided field assistance and good company: Kevin Akaoka, Tim Argast, Brett Eaton, Luke Gould, Greg Grzybowski, Eleri Harris, Cameron Hunter, Michele Koppes, Jason Leach, Alex McMahon, Dan Moore, Alexis Moyer, Tobias Müller, Elli Papangelakis, Robin Pike, Colin Sutherland, Charlotte Trowbridge, David West, and André Zimmermann.

Many of the field and laboratory experiments would not have been possible without the equipment and water samples provided by Jane Bachman (Environmental Dynamics, Inc.), Frank van der Have and Christoph Langley (Hoskin Scientific), Dave Hutchinson (Water Survey of Canada), Robin Pike (Ministry of Environment), Gabe Sentlinger (Fathom Scientific), and Northwest Hydraulic Consultants.

I would like to thank Professor Stephen Hauck at Case Western Reserve University and Professor Daniel Bain at University of Pittsburgh for introducing me to the wonderful world of environmental science and fluvial systems.

Lastly, I would like to thank my parents, sister and brother who have supported me throughout my education, and are always keen to learn about my thesis work.

Chapter 1

Introduction

1.1 Motivation for the study

In the last decade, there has been increasing attention within both the operational and research communities to quantifying the uncertainties in stream flow data (e.g. Liu et al., 2009; Westerberg et al., 2011; McMillan et al., 2012). Hydrologists need a clear understanding of the uncertainty associated with the data they are using for integration into rating curve development, hydrological model calibration, and hydrologic analyses. The uncertainty associated with a discharge time series combines the uncertainties in the discharge measurement, in the measurement of stage, and in the rating curve. This study focuses on discharge measurement uncertainty. Field discharge measurements may be prone to high uncertainty, and factors that affect uncertainty include field conditions, practitioner experience, and the method used for discharge measurement.

The velocity-area method via current metering or via acoustic doppler current profiling is the most commonly used method for discharge measurement. There is a vast body of literature exploring the accuracy of, and the uncertainties associated with, the velocity-area method (e.g. Herschy, 1975; Pelletier, 1988; Oberg and Mueller, 2007). However, this method may be impractical or subject to great uncertainties for steep stream reachs due to complex channel geometries.

An alternative discharge measurement method is dilution gauging via stream tracers (dominantly salt or Rhodamine dye). This method can be a powerful tool for measuring stream discharge or exploring solute dynamics, especially in steep, rough streams that cannot be gauged accurately using the velocity-area method (Moore, 2005). Dilution gauging has been growing in use due to increasing need to monitor discharge in steep mountain streams. For example, flow measurements in these streams are vital for planning and managing run-of-river hydro-electric projects that are typically sited on steep streams, and for scientific studies that focus on the hydrology of headwater streams (e.g. Gomi et al., 2002; Ward et al., 2013; Kelleher et al., 2013).

The advantage of dilution gauging over the velocity-area method for steep streams warrants further research into the uncertainty of dilution gauging. The method has been shown to be accurate to within ± 4-7% (Day, 1977) and is applicable to a wide range of stream sizes, from small first-order streams (Q = 0.007 m^3/s) to large rivers (Q = 400 m^3/s) (Gonalez-Pinzon et al., 2013).

Despite decades of experience with tracer injection, there are many uncertainties involved in the method. Furthermore, there are no standard operating procedures (SOPs) for tracer dilution gauging for discharge measurements, leading to the emergence of a range of different methodologies based on individual practitioner knowledge and experience. In contrast, SOPs have been developed for the velocity-area method of discharge measurement by different government agencies (e.g. Letvak et al., 1998; Turnipseed and Sauer, 2010).

Salt tracers and dye tracers are the most common conservative (non-reactive) tracers used in hydrology studies. Salt tracers tend to be more widely used for discharge measurements than dye tracers, but questions and concerns have been raised in the scientific literature and in the water resources industry, such as the magnitude of measurement uncertainty (Moore, 2005; Sentlinger et al., 2014[1]), the reliability of tracer experiments for developing relations between stream flow and flow resistance (e.g. Lee and Ferguson, 2002; Comiti et al., 2007), and the quantity of salt to inject during an experiment (Kite, 1993; Hudson and Fraser, 2002; Moore, 2005). Dye tracer injection methods, while more expensive than salt tracer methods, have the ability to measure higher discharges because dye concentrations are detectable at much lower concentrations than salt. However, many practitioners are hesitant to use dye tracers due to the potential for non-conservative behaviour and significant mass loss in the stream channel (Bencala et al., 1983; Clow and Fleming, 2008). Tracer dye is susceptible to in-channel loss due to sorption onto sediment suspended in the water and on the channel bed and photolysis from sunlight, so it may not be an appropriate method for highly turbid streams or for exposed streams on sunny days. Nevertheless, some practitioners have adopted dye methods exclusively, but the range of applicable scenarios is not widely known.

For a tracer dilution measurement, tracer material is injected into a stream and its concentration is monitored at a downstream location. The primary assumption of dilution gauging is that the tracer is completely mixed across the stream channel at the location of measurement. The stream reach distance required for complete mixing is the mixing length (x_m). The major processes that govern tracer transport and mixing are the bulk transfer of tracer material via advection downstream, transverse dispersion across the stream channel via turbulence, vertical mixing through the water column, and longitudinal dispersion that causes some material to travel downstream more quickly (Moore, 2005).

There are two injection techniques for discharge measurement via tracer dilution. Constant-rate

[1] Sentlinger, G., Zimmermann, A., Pike, R., Hutchinson, D., Hudson, R., Richardson, M., and Moore, R. Salt dilution standard operating procedure protocol working group meeting. April 29, 2014. Environment Canada, Vancouver, BC.

injection involves injecting a continuous supply of tracer material into the stream for the duration of the measurement, while slug injection involves a near-instantaneous injection of a specified amount of salt. Constant-rate injection tends to be more accurate, because complete mixing at the measurement location can easily be verified, the method only requires measurements at the stream water background tracer concentration and at the steady state tracer concentration, and long tracer residence times in the measurement reach do not affect the discharge measurement. However, slug injection may be more appropriate at higher flows since less tracer material is needed. Also, specialized equipment is needed for constant-rate injection; therefore, slug injection may be preferred due to equipment availability, costs, and/or site accessibility.

Slug injection will be the focus of this thesis due to its potential to measure a much wider range of discharges with significantly less tracer material and specialized equipment. For slug injection, the tracer can be injected in two ways. For slug injection via salt-in-solution, the salt is pre-mixed with stream water, and a known volume of this primary/injection solution is injected into the stream. For slug injection, a known mass of salt is injected directly into the stream, either as dry salt or as a brine comprising the known mass of salt and an arbitrary volume of water.

The record of tracer concentration with time at the measurement location is called a tracer breakthrough curve (BTC) (Figure 1.1). For salt tracers, the temperature-corrected electrical conductivity (EC_T) of the stream water is measured, as the difference between $EC_T(t)$ (the EC_T measured at time t ($\mu\text{S} \cdot \text{cm}^{-1}$)), and EC_{BG} (the background EC_T of the stream water ($\mu\text{S} \cdot \text{cm}^{-1}$)) is linearly related to the concentration of the injected salt. For dye tracers, the fluorescence of the stream water is measured.

The discharge (Q) of a stream can be determined from the integral of the BTC (approximated as a summation of discrete measurements) and the initial mass of injected salt, as follows:

$$Q = \frac{M}{CF_T \cdot \Delta t \sum_{i=1}^{n} [EC_T(t) - EC_{BG}]} \tag{1.1}$$

where M is the volume of salt injected (g), CF_T is a calibration constant relating salt concentration to EC_T ($\text{g} \cdot \text{cm} \cdot \mu\text{S}^{-1} \cdot \text{m}^{-3}$), Δt is the time interval between successive measurements (s), and n is the number of EC_T measurements. To determine the calibration constant CF_T, a solution of salt and water (known as the secondary solution) is added to a sample of stream water in increments. The resulting EC_T and salt concentration ($[NaCl]$) after each addition of secondary solution is recorded. $[NaCl]$ is plotted as a function of the EC_T, and the slope of the line, CF_T, is determined by linear regression.

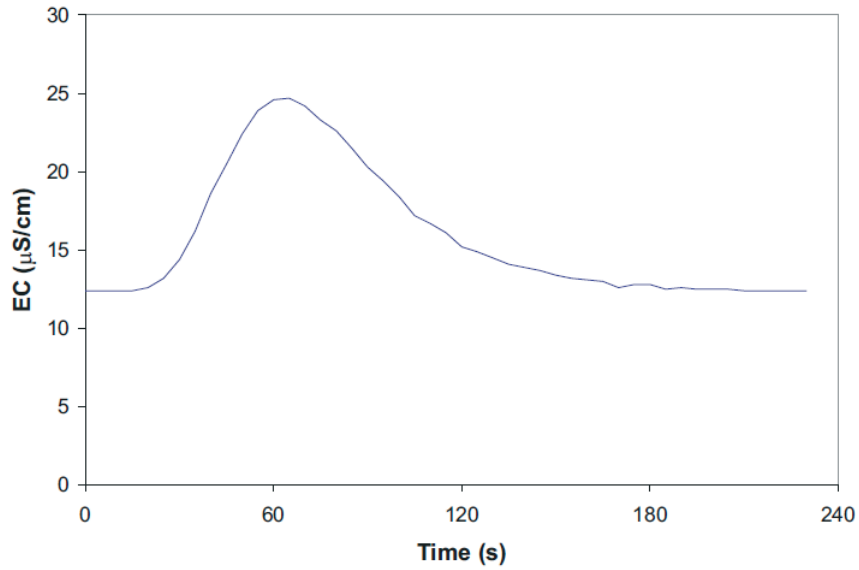

Figure 1.1: An example breakthrough curve (BTC) for a slug injection salt dilution discharge measurement.

The objective of this study was to contribute to our understanding of the uncertainties and limitations of, and best practices for, tracer dilution gauging by slug injection. Progress in this subject will save time and money for practitioners, promote consistency between different flow measurements, and improve confidence in the results of hydrological studies. The remainder of this chapter consists of a literature review identifying key knowledge gaps, followed by specific research objectives to address these knowledge gaps.

1.2 Literature review

1.2.1 Salt dilution gauging

In this section, the current state of knowledge of salt dilution gauging is reviewed with particular attention to three topics: (1) the calibration procedure, (2) determination of mixing length, and (3) estimation of appropriate mass of salt to inject.

Calibration procedure. The calibration procedure relating EC_T and $[NaCl]$ is a primary source of uncertainty in discharge measurements. The practitioner must decide how many additions of

secondary solution are sufficient to characterize the relation between $[NaCl]$ and EC_T. Different practitioners are known to use one, four, or more additions of secondary solution. Moore (2003) suggested to add secondary solution until the EC_T measured in the calibration tank exceeds the maximum EC_T recorded during the dilution measurement, in order to accurately characterize the range of EC_T values measured during passage of the breakthrough curve.

For the salt-in-solution method, the practitioner can use a volume of the primary/injection solution to determine the relation between EC_T and the relative concentration of injection solution in the stream water. Salt-in-solution is advantageous since it is only based on measurements of volume, which can be accurately measured in the field. However, since the secondary solution is based on the injection solution, the calibration procedure must be performed for each measurement. Also, if the salt concentration is unknown in the injection solution, and there is an error during the calibration procedure, the discharge measurement is invalid since one cannot simply re-calibrate with a different solution of differing salt concentration.

For the dry injection method, a calibration solution must be created with a known mass of salt mixed with water. Mass measurements are difficult in the field, and practitioners may bring pre-weighed salt to add to stream water for the secondary solution, or they may pre-mix a secondary solution. Practitioners may use stream water, distilled water, or tap water for this calibration solution. However, if the water used to generate the calibration solution differs from the background EC_T for the gauged stream, the calibration factor will be biased. For example, when using distilled water, the effective background concentration decreases with each addition of calibration solution due to dilution of the stream water with low-conductivity distilled water. The dry injection calibration procedure can be advantageous since the secondary solution is not dependent on the concentration of the injection solution, and a practitioner can use a standard secondary solution (e.g. 2.0 g salt in 1.0 L water) for every calibration.

A. Zimmermann (pers. comm., October 19, 2014) and G. Sentlinger (pers. comm., October 27, 2014) have each developed a correction procedure to account for differences in EC_T between distilled water used for the secondary solution and the stream water. However, a correction proce-

dure for calibration is not included as an SOP from any agency. An adequate correction procedure will allow practitioners to pre-mix a secondary solution before heading into the field, and to use one secondary solution for multiple tracer injections at different stream sites.

Mixing length determination. One of the most critical factors governing the accuracy of stream gauging by slug injection is the requirement that the tracer be fully mixed across the stream at the measurement location. A range of models have been proposed to determine mixing lengths based on hydraulic and geometric parameters of the stream (e.g. Glover, 1964), and the application of one-dimensional diffusion models (e.g. Fischer, 1966; Yotsukura and Cobb, 1972; Ward, 1973). Many of these early models proposed that the mixing length must be much longer for tracer injections from the side of the channel, x_s, versus injections from the centre of the channel, x_c. Glover (1964) and Fischer (1966) suggested that $x_s = 4 \cdot x_c$, while Ward (1973) suggested that $x_s = (25/7) \cdot x_c$.

Day (1977) studied mixing lengths on five mountain streams in New Zealand. The streams were described as steep (slope = 0.018 - 0.027 m/m), with large relative roughness values, and stream widths ranging from 2.7 m to 11.4 m. Based on results from 41 dilution gaugings, Day recommended that the mixing length (x_m) should equal or exceed 25 wetted stream widths (w) to ensure complete mixing. He also determined that centre versus side injection does not have a significant effect on the mixing length. Day's (1977) protocol remains the de-facto standard when estimating an adequate mixing length for a stream reach. However, the mixing characteristics of the stream will be dependent on its geomorphic properties as well as the flow level, suggesting that a universal mixing length ($x_m = 25 \cdot w$) may not be accurate for all streams and all flow levels. Furthermore, in some streams it may be impossible to find a suitable stream reach that is long enough to accomodate Day's standard (e.g. due to tributary inflow, safety/accessibility).

An adequate mixing length is typically confirmed by comparing discharge measurements from two different measurement locations for the same tracer injection. If the measurements agree within some specified tolerance (based on the estimated uncertainty of the calculated discharges), then the mixing length is considered adequate. Ideally, the measurement locations are on opposite sides of the stream. With this method, however, it can be difficult to determine the mixing length, often due

to surface-subsurface water fluxes. For example, Zellweger et al. (1989) found that, for a gravel-bed stream, measured discharge increased as the measurement location moved downstream, because the tracer needed a longer stream reach to fully mix with sub-channel bed flow. Clow and Fleming (2008) also found a steady increase in discharge measurement moving downstream, and attributed it to either surface-subsurface water fluxes or tracer loss. The measurement discrepancy arising from mixing length ambiguity poses a major issue for accurate stream flow measurements.

Tracer dosage for injection. The quantity of tracer to inject during an experiment is a balancing act, as there must be enough injected to ensure an adequate response for accurate measurements (Moore, 2005) while minimizing the potential for deleterious ecological impacts (Wood and Dykes, 2002). The minimum dosage necessary is dependent on the stability of the measurement reading, the precision of the measurement probe, the desired increase in tracer concentration, and the mixing characteristics of the stream. For example, a stream with less longitudinal dispersion induces a more concentrated salt wave with a higher peak concentration, and requires less injection volume (Moore, 2005). Multiple suggestions for minimum mass for injection have arisen in the literature and from personal communication (Table 1.1). Moore (2005) also suggested conducting trial injections with a small volume or mass, and then increasing the volume or mass as necessary.

Table 1.1: Salt dilution dosage guidelines from various sources.

Literature	Suggestion for peak EC_T (EC_{peak}) and/or injection amount
Kite (1993)	$EC_{peak} > 1.5 \cdot EC_{BG}$
Hudson and Fraser (2002)	$EC_{peak} > 6.0 \cdot EC_{BG}$
Moore (2005)	$EC_{peak} > 2.0 \cdot EC_{BG}$ to $3.0 \cdot EC_{BG}$ for streams with $EC_{BG} < 50$ μS/cm
	$EC_{peak} > 1.5 \cdot EC_{BG}$ for streams with $EC_{BG} > 50$ μS/cm
A. Zimmermann (pers. comm., July 31, 2015)	$EC_{peak} > EC_{BG} + 30$ μS/cm
	1 kg of salt per m^3/s of stream flow, or 0.5 kg of salt per m^3/s of stream flow for well-mixed channel with minimal in-channel storage
B. Bowden (pers. comm., August 5, 2015)	Consider BTC as square pulse at easily measureable concentration. Injection mass is based on this concentration and expected stream discharge

1.2.2 Rhodamine WT dye dilution gauging

Rhodamine WT (RWT) is the most commonly used dye for measuring discharge via tracer dilution. In-channel tracer loss is a major concern for Rhodamine WT, due to its ability to sorb to organic and inorganic material in suspension or in the bed, and photolysis. Tracer loss (via decay or other processes) would cause an overestimate of discharge, since the tracer would be more diluted in the stream water. Also, light scattering by suspended sediment may affect the measured fluorescence.

Smart and Laidlaw (1977) looked at tracer properties for seven different fluorescent dyes, including RWT, in a series of laboratory experiments. Notable findings from that study relating to RWT decay are as follows: (1) suspended sediment raised measured fluorescence and reduced effective dye fluorescence due to light absorption and scattering by the sediment, (2) sorption effects were not found to be an issue for sediment concentrations below 1000 mg/L, unless the sediment was very fine and/or contained organic matter, and above 1000 mg/L adsorption became a potential issue, (3) dye losses did not scale proportionally with the amount of dye, and therefore the percentage loss in dye was relatively higher for low concentrations than for high concentrations.

Researchers conducting field studies with RWT have reported effects from sediment sorption and photolysis. Duerk (1983) did not find significant dye loss from any source when they gauged two concrete-lined storm sewers during a series of rain events. Bencala et al. (1983) found (1) tracer loss due to interaction with the gravel stream bed (the stream water had low suspended sediment concentration), (2) no interaction between salt and RWT in a laboratory experiment, and (3) evidence of RWT sorption to suspended sediment in a laboratory experiment. Dierberg and DeBusk (2005) found tracer loss due to sediment adsorption and photolysis. However, it is important to note that the field and laboratory experiments performed by Bencala et al. (1983) and Dierberg and DeBusk (2005) were over much longer time scales (multiple hours to multiple days) than are the case for dilution gauging injections (typically under an hour for the tracer to flush out of the stream reach). Kilpatrick and Cobb (1985) suggested that significant RWT decay from photolysis occurs when exposed to direct sunlight for several hours.

These studies have confirmed that (1) RWT decay due to sediment sorption and photolysis is a

possible issue, and (2) suspended sediment affects the measured fluorescence. However, no studies known to the author have focused specifically on the effect that RWT decay or suspended sediment concentration has on a dilution discharge measurement.

1.3 Research objectives and thesis structure

The review in Section 1.2 has identified a number of knowledge gaps in the current protocols for tracer dilution gauging for stream discharge measurements. The overall objective of this study was to improve current field and analysis techniques for tracer dilution gauging, as we move towards the development of standard operating procedures to measure stream discharge. The specific research questions addressed by the thesis are:

1. For salt dilution gauging via injection of dry salt, what are the uncertainties associated with the range of calibration procedures currently in use, and what is the most accurate and robust approach to calibrating the relation between salt concentration and electrical conductivity? To what extent does the calibration factor vary with background water chemistry? How much uncertainty would be involved in using a standard value if it is not possible to conduct a calibration in the field?

2. For Rhodamine WT dilution gauging via injection of dry Rhodamine WT, to what extent does the calibration factor vary with suspended sediment concentration (turbidity level)? How much uncertainty would be involved in using a standard value if it is not possible to conduct a calibration in the field, and how does this compare to the uncertainty for a standard value for salt calibration?

3. Can mixing lengths be predicted from geomorphic properties of the stream channel? What factors influence our ability to determine an adequate mixing length for a stream reach?

4. How sensitive is the discharge measurement to location along or across the stream channel?

5. For salt dilution gauging, can dosage guidelines be developed based on geomorphic and/or geometric properties of the stream channel and desired increases of peak EC_T over background

EC_T?

6. For gauging with Rhodamine WT, what are the effects of tracer decay (from sorption and photolysis) on the calibration procedure and discharge measurement?

The remainder of this thesis is organised as follows. Chapter 2 describes the study sites and the field, laboratory, and data analysis methods. Chapter 3 presents results of the field experiments, laboratory experiments, and data analysis. Chapter 4 discusses the results in the context of the research objectives defined above. Chapter 5 summarizes the main conclusions of this study, presents recommendations for SOPs, and identifies areas where further research is required.

Chapter 2

Study sites and methodology

2.1 Study sites

2.1.1 Field sites

The study focused on streams that are appropriate for stream gauging via tracer dilution. These streams are small to intermediate size (typical discharges less than 10 m^3/s) with gradients exceeding 2% and channel morphologies ranging from riffle-pool to cascade (Table 2.1, Figure 2.1). Study streams were located in the southern Coast Mountains and Vancouver Island (Figure 2.2).

Table 2.1: Streams used in study

Stream	General location	Coordinates (approximate)	Channel type	Average slope (%)	Average channel width (m)	Discharge (m^3/s)	Average flow velocity (m/s)	No. reaches
Bridge Glacier South Creek	Lilloet Icefield,	50°49' 50" N 123°29' 50" W	Step-pool	5.7-22	6-8*	0.78-3.58	0.30-1.08	5
Bridge Glacier West Creek	Lilloet Icefield,	50°49' 47" N 123°33' 19" W	Step-pool	9.5	10-12*	4.58-10.8	0.73-1.02	1
Carnation Creek Tributary C	Southwest Vancouver Island	48°55' 05" N 124°59' 02" W	Riffle-pool	1.9	3.9	0.010-0.188	0.06-0.36	1
Carnation Creek Tributary L	Southwest, Vancouver Island	48°55' 05" N 124°59' 02" W	Step-pool	8.6	2.1	0.009-0.010	0.07-0.08	1
Cayoosh Creek	Pemberton	50°23' 05" 122°28' 10"	Step-pool	10.7	6.1	4.50-4.96	0.86-0.89	1
Mosquito Creek	North Vancouver	49°21' 10" N 123°05' 6.5"	Step-pool	10**	5-7*	0.261-0.319	0.23-0.28	1
Pemberton Creek	Pemberton	50°19' 19" N 122°48' 44" W	Cascade-pool	4.1	8.9	1.10-3.93	0.45-0.75	1
Place Creek	Pemberton	50°27' 57" N 122°38' 31" W	Step-pool (steep)	18	7.1	0.542-1.03	N/A	1
Rutherford Creek	Between Whistler and Pemberton	50°16' 19" N 122°52' 13" W	Cascade-pool	3.4	7.7	1.77-3.04	0.41-0.48	2

* indicates estimates made from field photographs
** indicates estimate made from Google Earth

(a) Place Creek

(b) Rutherford Creek

(c) Pemberton Creek

(d) Carnation Tributary C

(e) Carnation Tributary L

(f) Mosquito Creek

(g) Bridge Glacier South Creek

(h) Bridge Glacier West Creek

(i) Cayoosh Creek

Figure 2.1: Streams used in study

2.1.2 Water sample sites

Water samples were collected at field sites listed in Table 2.1, at Northwest Hydraulic Consultants (NHC) project sites, at Environmental Dynamics Inc. project sites, and at Water Survey of Canada hydrometric gauging stations (Figure 2.2). The intention was to collect a diverse set of water samples from different areas of British Columbia and Yukon with a range of background water chemistry and electrical conductivity. Samples were collected in 1-L plastic sample containers and transported

to NHC. They were stored in a refrigerator to keep them near in-situ temperature until they were calibrated.

2.2 Field methods

2.2.1 Stream gauging for salt dilution

Tracer injections were performed to determine stream discharges as well as study the mixing dynamics of the streams. The dry mass slug injection method (Hudson and Fraser, 2005) and the salt-in-solution slug injection method (Moore, 2005) were used. Dry injection was used for higher flows when more salt was needed and rapid dissolution of the salt could be ensured. Slug injection with salt-in-solution was used for lower flows. In general, these methods are the preferred measurement techniques for the study streams, as the stream reaches are high-gradient and turbulent, facilitating rapid mixing of solutes.

Dry mass injection is performed by injecting a known mass of salt upstream and measuring the change in temperature-corrected electrical conductivity (EC_T) at a point downstream of the injection point. Prior to injection, the background EC_T (EC_{BG}) of the ambient streamwater is measured. After injection, EC_T is measured as the salt wave travels downstream, until the EC_T returns to its stable, background level.

A calibration procedure relating mass concentration of the salt to the EC_T of the water was performed either on-site or later in the laboratory with a collected stream water sample. First, the background EC_T of the streamwater is measured. Then, a salt solution (typically 2 g of salt in 1 L of streamwater, known as the secondary solution) is added in either 5 or 10 mL increments, and the new EC_T is recorded after each secondary solution addition followed by stirring to ensure it is fully mixed into the stream water sample. The stream water sample with the additional secondary solution is known as the calibration solution. Secondary solution additions are continued until the EC_T of the calibration solution exceeds the maximum EC_T observed during the injection. The salt concentration of the calibration solution is plotted as a function of the EC_T of the calibration solution, and the slope of the line is determined by linear regression. The slope of this relation is

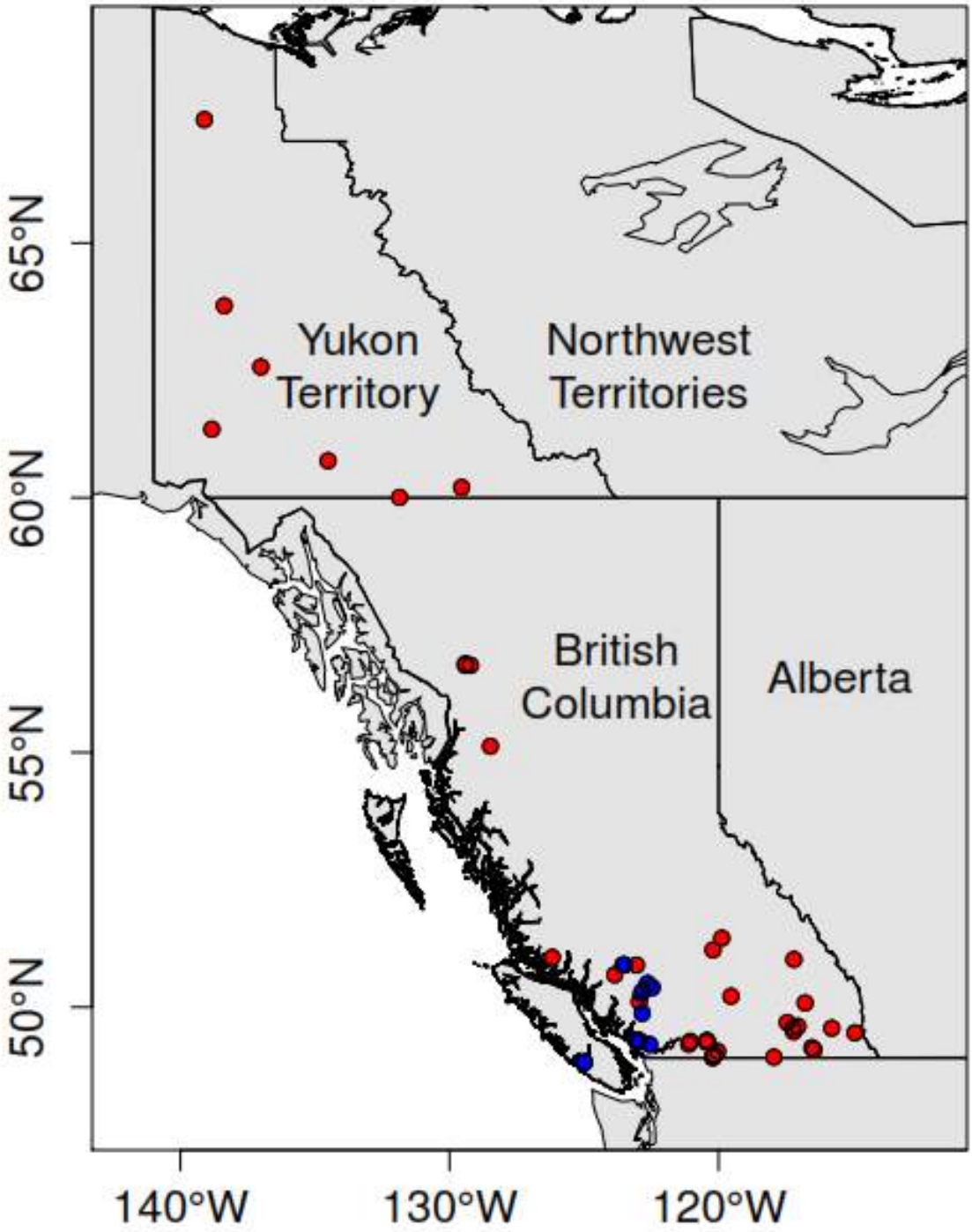

Figure 2.2: Field sites and water sample sites: fieldwork and water sample acquired (blue dots) and water sample only (red dots). Five additional water sample sites were in Yukon, but the exact locations are unknown.

referred to as temperature-corrected calibration factor, CF_T ($\mathrm{g \cdot cm \cdot \mu S^{-1} \cdot m^{-3}}$).

After calibration, the stream discharge, Q ($\mathrm{m^3/s}$), can be calculated as

$$Q = \frac{M}{CF_T \cdot A} \tag{2.1}$$

where M is the mass (g) of salt injected into the stream, and A is the area under the plot of EC_T - EC_{BG} versus time ($\mathrm{\mu S \cdot s \cdot cm^{-1}}$). The value of A is typically determined as follows:

$$A = \Delta t \cdot \sum_{i=1}^{n} [EC_T(t) - EC_{BG}] \tag{2.2}$$

For salt-in-solution injection, a primary solution is made with salt and stream water. A typical concentration for the primary solution is 1 kg of salt in 6 L of water, or about 160 g/L, which is sufficiently below the solubility to ensure complete dissolution of the salt (Moore, pers. comm.). A sample of primary solution, typically 50 or 100 mL, is removed and set aside for calibration. A measured volume of primary solution is injected into the stream at the injection point, and EC_T is monitored in the same way as dry injection.

The primary solution set aside for calibration is diluted in a secondary solution by mixing a small volume of primary solution (typically 5 or 10 mL) with a sample (typically 1.0 L) of pure stream water. This secondary solution is incrementally added to a streamwater sample and changes in EC_T are recorded in the same manner as the dry injection method.

After calibration, the stream discharge can be calculated as

$$Q = \frac{V}{k_T \cdot A} \tag{2.3}$$

where V is the volume (L) of primary solution injected into the stream, and k_T is the slope of the calibration line ($\mathrm{L \cdot cm \cdot \mu S^{-1} \cdot m^{-3}}$).

Electrical conductivity was measured using two instrument setups. The first setup is a WTW Multi 340i handheld meter connected to a Cambell Scientific CR510 data logger. The data logger is set up to measure EC_T at 1-s intervals, and record a 5-s average of these measurements. The WTW

meter is accurate to ± 0.1 µS/cm for EC_T readings below 200 µS/cm, and accurate to ± 1 µS/cm for readings above 200 µS/cm. The second setup is a high-resolution electrical conductivity sensor (H-RECS) connected to a QiQuac storage device, developed by Aquarius Research & Development. The QiQuac measures EC_T at 1-s intervals and records a 6-s average of these measurements. The H-RECS is accurate to 0.01 µS/cm.

The electrical conductivity (EC) of water increases with temperature. All measurement probes compensate for this by applying a nonlinear correction to the measured electrical conductivity based on the measured temperature. This results in the temperature-corrected electrical conductivity (EC_T), which is the equivalent EC value at 25 °C.

2.2.2 Measurement probe setup

The EC_T measurement probes were set up in three arrangements, depending on whether the goal was to measure discharge, to study mixing lengths, or to study variability of breakthrough curves and discharge measurements with measurement location (Figure 2.3). To assess whether the salt was completely mixed at the downstream end of the reach, two probes were set up on opposite sides of the stream, and staggered downstream by 5 to 10 m. When access to both sides of the stream was not possible, the probes were staggered on the same side of the stream. Complete tracer mixing in the stream channel was assumed if the two measurements agreed within a reasonable tolerance.

To study mixing lengths, complete mixing was first verified by comparing discharges determined from two probes placed as described earlier. These first two probes were typically located at least 25 wetted widths downstream, the recommendation of minimum reach length from Day (1977). Additional probes were installed upstream in a longitudinal pattern.

To study variability associated with measurement location, complete mixing was first verified by comparing discharges determined from two probes placed as described earlier. In subsequent measurements, probes were placed downstream of the point of complete mixing in different areas of the stream. Figure 2.3d shows an example probe setup for measurement location variability, where probes were placed in a slow-moving side pool (Probe 3), in a backwater eddy behind an obstruction

(Probe 2), in a flow constriction (Probe 1), or in turbulent whitewater (Probe 4). In some scenarios, the probes were placed in close proximity to minimize the effects of longitudinal dispersion of the tracer as much as possible. In other scenarios, some probes were placed significantly further downstream (up to 54 wetted widths) to observe the effects of extending the reach length.

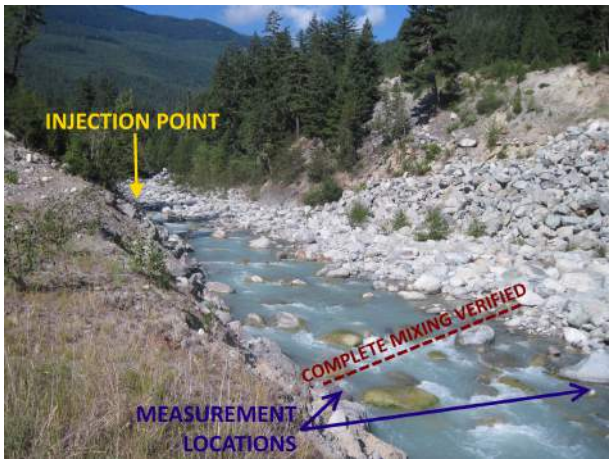

(a) Discharge measurement setup

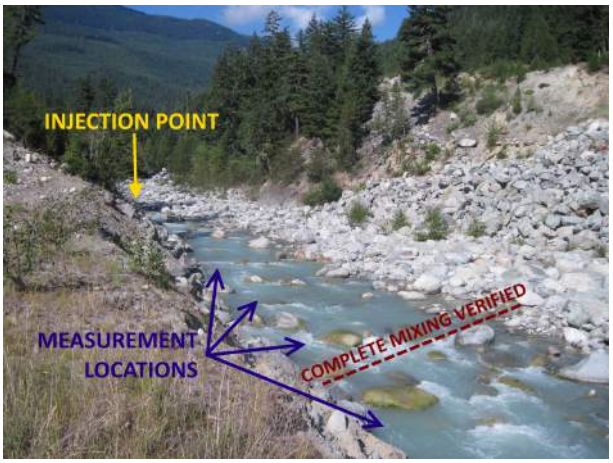

(b) Mixing length setup

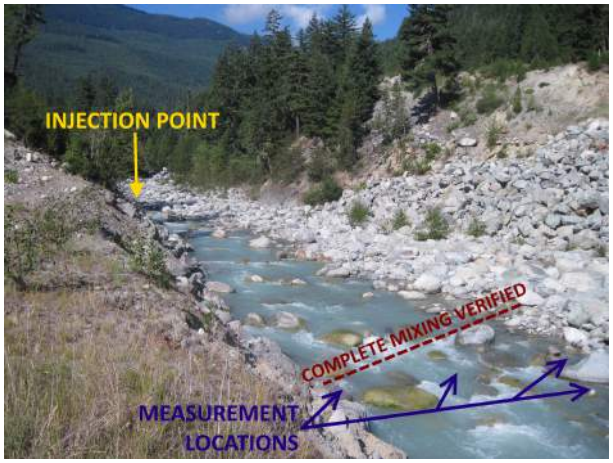

(c) Microscale variations setup

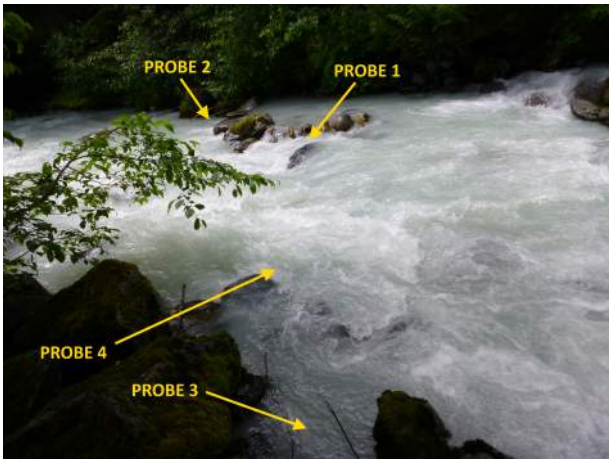

(d) Microscale variations setup, close up on measurement locations

Figure 2.3: Examples of experimental setups at Rutherford Creek (a, b, c) and Pemberton Creek (d). For reference for Rutherford Creek, the distance from the injection point to the location where complete mixing was verified was 140 m and the mean wetted width was 7.7 m. For reference for Pemberton Creek, the mean wetted width was 10.0 m.

2.2.3 Surveying

Channels were surveyed to determine reach length, reach gradient, average wetted channel width, and a classification of channel morphology. Reach length was measured with a surveyor's tape or a LTI TruPulse 360R rangefinder (specified accuracy from manufacturer for distance measurements is $\pm$ 30 cm). Reach gradient was calculated using reach length measurements and vertical distance measurements with the rangefinder. Average wetted channel width was measured with a surveyor's tape when the stream was small enough to wade across safely; otherwise, a rangefinder was used. Width measurements were taken at three to five locations along the stream reach and averaged. Distances were measured to the nearest 0.1 m. Channel morphologies were determined by visual observation in the field and from photographs. These observations were matched to specific morphologies detailed in the BC Channel Assessment Procedure Field Guidebook (British Columbia, 1996). The morphologies in Table 2.1 refer to the classifications in the Field Guidebook.

2.2.4 Stream gauging for Rhodamine WT dye dilution

Stream gauging with Rhodamine WT dye follows the same principles as salt dilution gauging. A known mass of RWT was injected upstream and the change in dye concentration was measured downstream of the injection point. The fluorescence probe provided output in millivolts (mV). A calibration procedure, analogous to salt dilution calibration, was performed to relate Rhodamine WT concentration (g/L) to measurements in mV.

After calibration, the stream discharge Q (m^3/s) can be calculated as

$$Q = \frac{M}{CF_R \cdot A} \tag{2.4}$$

where M is the mass (g) of Rhodamine WT dye injected into the stream, CF_R is the slope of the calibration line ($\mathrm{g} \cdot \mathrm{L}^{-1} \cdot \mathrm{mV}^{-1}$), and A is the area under the plot of $RWT(t)$ - RWT_{BG} versus time ($\mathrm{mV} \cdot \mathrm{s}$), where $RWT(t)$ is the measurement reading from the fluorometer at time t (mV), and RWT_{BG} is the measurement reading from the fluorometer for the ambient stream water (mV) .

Discharge measurements with RWT were performed at Mosquito Creek in North Vancouver,

BC. Two dye probes were placed downstream of complete mixing (215 m from injection point), and two additional probes were placed much further downstream (520 m from injection) to observe any effects of sorption to suspended sediment or the stream channel. Each dye probe had a conductivity probe installed in close proximity. For each injection, dye was injected into the stream, followed by a salt injection approximately three minutes later. This procedure allowed for comparison between the two tracer dilution techniques. Laboratory experiments have shown that salt and RWT do not interact (Bencala et al., 1983), allowing for concurrent tracer measurements.

For Rhodamine gauging, Sommer TQ-Tracer fluorescent tracer devices were used. These devices record measurements at 1-s intervals, and are accurate to ± 0.1 mV. The instrument setup for the salt dilution was the same setup as described in Section 2.2.1.

2.3 Laboratory methods

2.3.1 Laboratory calibrations for salt dilution

Laboratory calibrations to determine the temperature-corrected calibration factor (CF_T) for salt dilution gauging were performed at Northwest Hydraulic Consultants (NHC) in North Vancouver, British Columbia. The calibration procedure is the same as described in Section 2.2.1 above.

Five comparative experiments, in conjunction with data provided by NHC, were performed to observe CF_T variation due to equipment, calibration procedure, the technician performing the calibration, and the environment in which the calibration was performed (Table 2.2). Table 2.3 lists the equipment and materials used for laboratory calibrations.

The environmental setup and procedures were intended to be as controlled as possible to minimize experimental and human error. Volumetric flasks, mason jars, and probes were rinsed with distilled water and stream water prior to calibration. Stream water and standard calibration solutions were mixed vigorously before each calibration. At each addition of standard solution into the calibration stream water, the water was mixed until the EC_T reading stabilized. When calibrating at in-situ stream temperature, the calibration stream water and standard solution were placed in an ice-water bath to keep water temperature low (5-10 °C).

Table 2.2: Laboratory experiments for salt dilution calibration procedure

Experiment	Methods compared	Method (a)	Method (b)
1	(a) Autopipette vs. (b) Glass pipette	Autopipette used to inject secondary solution into stream water sample	Glass pipette used to inject secondary solution into stream water sample
2	(a) One secondary solution vs. (b) Multiple secondary solutions	One secondary solution used for all calibrations	New secondary solution used for each calibration
3	(a) Stream water vs. (b) Distilled water	Stream water mixed with NaCl used for secondary solution	Distilled water mixed with NaCl used for secondary solution
4	(a) In-situ temperature vs. (b) Room temperature	Calibrations performed at near in-situ temperature (ice bath)	Calibrations performed at room temperature
5	Comparing calibration results of various stream waters collected throughout British Columbia and Yukon		

Table 2.3: Instruments and materials used for laboratory calibrations for salt dilution

Equipment/Materials	Desciption/Information	Instrument precision
Sifto Hy-Grade Food Grade Salt		
Cole-Parmer Symmetry (120g x 0.0001g) mass scale		0.00005%
WTW Cond 3310	cell constant = 0.475 cm^{-1}	0.5%
Portable Conductivity Meter		
Tetracon 325 Conductivity Cell		0.5%
Thermo-Scientific Finnpipette F2 adjustable autopipette		0.8%
10 mL glass pipette		0.2%
Glass volumetric flask (500 mL)		0.0003%
Glass volumetric flask (1000 mL)		0.0004%
Two mason jars	For holding secondary solution and calibration solution	
Portable cooler and ice	For ice bath set-up in Experiments 4, 5	
PC software for salt gauging calibration	Developed in-house at NHC	
Distilled water	Used for secondary solution in Experiments 3, 4, 5	
Stream water (Seymour Creek, North Vancouver, BC)	Used for secondary solution in Experiments 1, 2, 3	
Stream water (Seymour Creek)	Water to be calibrated in Experiments 1, 2, 3	
Stream water (streams throughout BC)	Water to be calibrated in Experiment 5	

For Experiments 3 and 5, distilled water was mixed with salt to use for the secondary solution. Since the EC_{BG} of distilled water was different than EC_{BG} of the stream water to be calibrated, a distilled water correction must be applied. The effective EC_{BG} of the calibration stream water as secondary solution is added, $EC_{BG,eff}$, can be calculated as follows (Zimmerman, pers. comm.):

$$EC_{BG,eff} = \frac{EC_{BG,S} \cdot V_S + V_D \cdot EC_{BG,D}}{V_T} \tag{2.5}$$

where $EC_{BG,S}$ is the EC_{BG} of the stream water sample, V_S is the volume of the stream water sample, V_D is the volume of secondary solution added, $EC_{BG,D}$ is the EC_{BG} of the distilled water, and V_T is the total volume of the stream water sample and secondary solution added. Table 2.4 shows the results from an example calibration procedure, with and without the distilled water correction. The difference in CF_T values will increase as the difference of $EC_{BG,S}$ and $EC_{BG,D}$ increases. The correction from Equation 2.5 can be used with any secondary solution water (e.g. distilled water, tap water), as this would only change the value of $EC_{BG,D}$.

Table 2.4: Example calibration results using the distilled water correction used in this study. The concentration of the secondary solution was 1.99 g/L, the volume of stream water to be calibrated was 0.5 L, and the EC_T of the distilled water used for the secondary solution was 2.0 $\mu S \cdot cm^{-1}$.

Secondary solution added (L)	Salt concentration of calibration water (mg/L)	$EC_{BG,S}$ ($\mu S \cdot cm^{-1}$)	$EC_{BG,eff}$ ($\mu S \cdot cm^{-1}$)	EC_T measured ($\mu S \cdot cm^{-1}$)	EC_T corrected ($\mu S \cdot cm^{-1}$)
0	0.0	84.7	84.7	84.7	84.7
0.005	19.7	84.7	83.9	124.9	125.7
0.010	39.0	84.7	83.1	163.8	165.4
0.015	58.0	84.7	82.3	202	204.4
0.020	76.5	84.7	81.5	239	242.2
			Resulting CF_T ($g \cdot cm \cdot \mu S^{-1} \cdot m^{-3}$)	0.496	0.486

For Experiments 1-4, seven calibrations were performed for each method. The mean and standard deviation were determined for each method. A two-sided T-test for means and an F-test for variances were conducted to compare the two methods for each experiment. For Experiment 5,

many water samples were calibrated with one measurement probe. In addition, some water samples were calibrated with three probes concurrently to observe differences in probes. All measurement probes used were calibrated with a 0.01 mol/L KCl conductivity standard solution prior to stream water calibration.

Selected water samples from Experiment 5 were analyzed at the Ministry of Environment Analytical Laboratory. Samples were chosen based on unique characteristics such as low or high background EC_T and low or high CF_T value. The Analytical Laboratory performed cation analysis by ICP/OES Spectrometer and anion analysic by ion chromatography.

2.3.2 Laboratory calibrations and laboratory experiment for Rhodamine WT dye dilution

Laboratory calibrations for Rhodamine WT dye were performed to observe differences in CF_R due to suspended sediment concentration. Two TQ-Tracer devices were used for calibration at a low and high turbidity level. The turbidity sensor used was an Analite NEP395 Turbidity Probe, accurate to $\pm$ 0.1 NTU for turbidity measurements up to 400 NTU. Stream water from Seymour Creek (North Vancouver, BC) was used for the low turbidity calibration water (turbidity = 2.0 $\pm$1.0 NTU). Silt was added to the stream water to obtain a high turbidity calibration water (turbidity = 250 $\pm$ 50 NTU). At each addition of Rhodamine WT secondary solution, the measured fluorescence was recorded after 10 s of stirring of the calibration solution due to initial instability of the measurement signal. Before each addition of secondary solution, the turbidity of the calibration solution was measured and recorded. Seven calibrations were performed for each combination of probe (WSC_A and WSC_B) and turbidity level (low and high) for a total of four combinations. F-tests for variances were conducted to compare the variation of CF_R values between probes or between turbidity levels, and a two factor analysis of variance (ANOVA) was conducted to determine if there was a significant difference in average CF_R value between probe and between turbidity level.

For the laboratory experiment, low turbidity stream water (Seymour River, turbidity $<$ 10 NTU, volume = 19.5 L) in a large bucket was continuously mixed with a paint mixer connected to a drill press (Figure 2.4). Silt (from natural sources) and Rhodamine WT dye and were added throughout

the experiment to observe changes in both turbidity level and Rhodamine WT concentration. The experimental setup was covered with black bags to minimize light disturbance. Two RWT probes and the turbidity probe were installed securely in the water, with ample space between the measuring cells and the edges of the container.

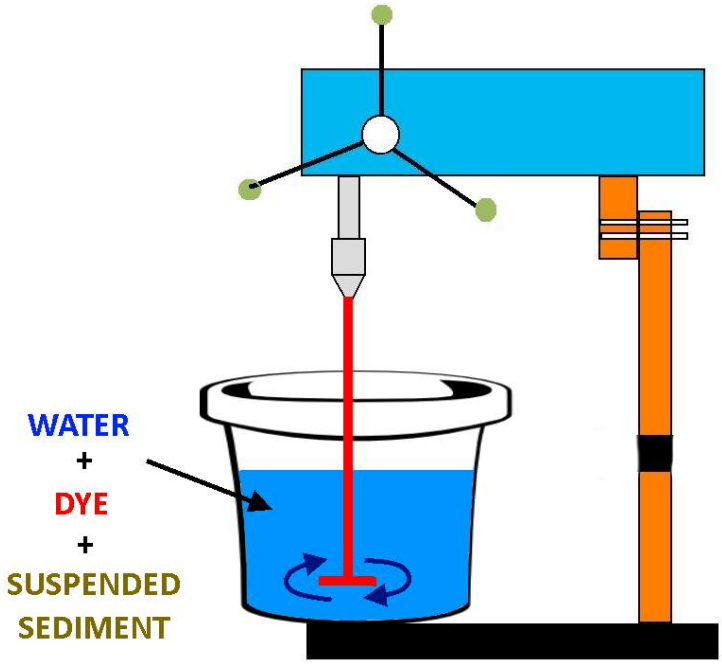

Figure 2.4: Rhodamine WT laboratory experiment setup

2.4 Data analysis

Data analysis was performed using the R programming language Version 3.1.3, in the RStudio IDE Version 0.98.1103 (R Core Team, 2015). Basic data organization and editing were done in Microsoft Excel 2013 and LibreOffice Calc.

2.4.1 Uncertainty analysis of discharge measurements

The uncertainty in stream discharge determined from dilution gauging has three components: the mass (or volume) or salt injected, the area under the breakthrough curve, and the calibration factor. Figure 2.5 shows a breakdown of the uncertainty associated with two example discharge measure-

ments.

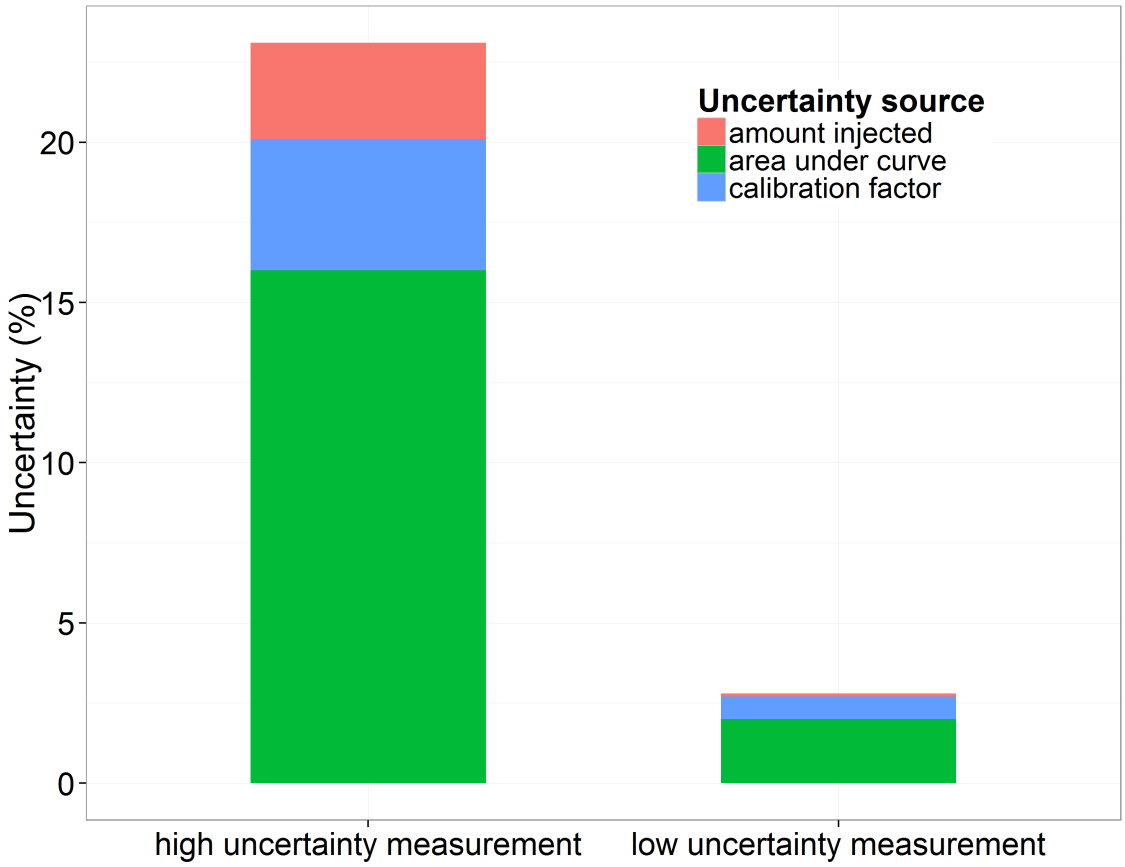

Figure 2.5: Discharge measurement uncertainty breakdown for a a typical low uncertainty measurement and a typical high uncertainty measurement.

If the salt is weighed before injection, the uncertainty of mass injected, δ_{mass}, is the resolution of the mass scale (typically 0.1 g). For some injections, unweighed boxes with nominal salt masses (1.0 kg or 1.8 kg) were injected. In this case, multiple boxes of salt were weighed, and the uncertainty was taken as two times the standard deviation of the measured mass.

The uncertainty associated with the area under the breakthrough curve, δ_A, is determined by

$$\delta_A = 2 \cdot n \cdot \sigma \tag{2.6}$$

where n is the number of EC_T measurements during the experiment, and σ is the measure of the

stability of the EC_T reading. If the recorded EC_T is completely stable, then σ is the resolution of the probe (typically 0.01, 0.1 or 1 µS/cm, depending on the equipment and range of EC_T values, see section 2.2.1). Each measurement point has two sources of uncertainty: the measurement itself and the background EC_T subtracted from the measurement, thus the multiplication by two.

The uncertainty in CF_T, δ_{CF_T}, is based on the variability of the CF_T values measured in this study. Two different values of δ_{CF_T} were used in this study, depending on how the calibration procedure was performed. If the stream water was calibrated by the author, then the value of δ_{CF_T} was based on the repeatability of the calibration (i.e. how much the CF_T varies between calibrations of the same stream water and same environmental conditions). Therefore, it was taken as two times the standard deviation of the seven calibrations performed for Experiment 1(a), described in Section 2.3.1. If the calibration was not performed and the CF_T was estimated, then the value of δ_{CF_T} was assigned a value of two times the standard error of the residuals of the relation between CF_T and EC_{BG} from Experiment 5 (Section 2.3.1).

The total uncertainty in a discharge measurement can be expressed either in terms of a maximum probable error (usually at a 95% confidence level) or a maximum possible error. These are calculated using the fractional error for each term. The maximum probable fractional error is calculated as

$$\frac{\delta_{dp}}{Q} = \sqrt{\left(\frac{\delta_{mass}}{M}\right)^2 + \left(\frac{\delta_A}{A}\right)^2 + \left(\frac{\delta_{CF_T}}{CF_T}\right)^2} \tag{2.7}$$

whereas the maximum possible fractional error is calculated as

$$\frac{\delta_{dm}}{Q} = \frac{\delta_{mass}}{M} + \frac{\delta_A}{A} + \frac{\delta_{CF_T}}{CF_T} \tag{2.8}$$

The values of δ_{dp} and δ_{dm} can be multiplied by the discharge (Q) to obtain the errors in units of discharge (m^3/s).

2.4.2 Mixing lengths

The maximum probable and maximum possible errors are used as tolerance ranges for each measurement. For individual discharge measurements, if the discharge measured upstream agreed with the furthest downstream discharge measurement, within the tolerance range, then it was deemed that complete mixing had occurred at the location of the upstream probe.

2.4.3 Relationships for dosing guidelines

As defined earlier, the equation to determine discharge from a dry salt injection is

$$Q = \frac{M}{CF_T \cdot A} \tag{2.9}$$

The area under the breakthrough curve, A, can be represented in non-dimensional form as

$$A^* = \Delta\tau \cdot \sum_{i=1}^{n} \phi_i \tag{2.10}$$

where ϕ is the normalized difference between EC_T and EC_{BG}, computed as

$$\phi = \frac{EC_T - EC_{BG}}{EC_{peak} - EC_{BG}} \tag{2.11}$$

and $\Delta\tau$ is one timestep of a non-dimensional time, τ, computed as

$$\tau = \frac{t}{t_h} \tag{2.12}$$

where t_h (s) is the harmonic mean travel time of the tracer pulse. Combining Equations (2.9) and (2.10) and re-arranging yields the following relation:

$$M = Q \cdot CF_T \cdot A^* \cdot t_h \cdot (EC_{peak} - EC_{BG}) \tag{2.13}$$

Since t_h is equal to the reach length, L (m), divided by the mean velocity, $\bar{v}$ (m/s), and Q divided by $\bar{v}$ is equal to the mean cross sectional area of the stream channel, A_c, Equation 2.13 becomes

$$M = A_c \cdot L \cdot A^* \cdot CF_T \cdot (EC_{peak} - EC_{BG}) \tag{2.14}$$

This relation indicates that the appropriate mass of salt to inject can be estimated given estimates or measurements of L, A_c, CF_T and A^*, and a desired change in EC_T from background to peak is specified. The derived relation in Equation 2.14 is algebraically equivalent to the RWT dosage suggestion reported by Kilpatrick (1970) that relates the volumetric RWT dosage to the desired peak RWT concentration.

To determine A^*, each BTC must be transformed with τ and ϕ. For this study, 121 discharge measurements from the field studies and 54 discharge measurements from fieldwork performed by Northwest Hydraulic Consultants (NHC) were analyzed to determine A^*. The distribution of values of A^* was used to determine recommended values for use in salt dosing calculations.

Chapter 3

Results

3.1 Calibration factors for salt dilution via dry slug injection

Summaries of the means and standard deviations for the first four experiments are provided in Table 3.1. As shown in Table 3.2, there are statistically significant differences in the mean CF_T between the use of an autopipette versus a glass pipette (Experiment 1), using one secondary solution versus a new secondary solution for each calibration (Experiment 2), and calibrating at room versus in-situ temperature (Experiment 4). The percent differences between the (b) method and the preferred (a) method were 0.5%, 0.3% and 1.3% for Experiments 1, 2, and 4, respectively. There were no significant differences among the variances for any of the experiments.

Table 3.1: Results from laboratory experiments for salt dilution calibration procedure

Experiment	Method	Sample size	Mean CF_T [(mg/L) / (μS/cm)]	Standard deviation of CF_T [(mg/L) / (μS/cm)]	Coefficient of variation
Experiment 1	(a) Autopipette	7	0.4750	0.001604	0.33%
	(b) Glass pipette	7	0.4774	0.001386	0.29%
Experiment 2	(a) One secondary solution	7	0.4750	0.001604	0.33%
	(b) Multiple secondary solutions	7	0.4765	0.000717	0.15%
Experiment 3	(a) Stream water secondary solution	7	0.4750	0.001604	0.33%
	(b) Distilled water secondary solution	7	0.4748	0.000687	0.14%
Experiment 4	(a) In-situ temperature calibration	7	0.4811	0.000927	0.19%
	(b) Room temperature calibration	7	0.4748	0.000687	0.14%

In Figure 3.1, the CF_T values of the water samples are plotted in black and blue for the province-

Table 3.2: Statistical tests for laboratory experiments for salt dilution calibration procedure. There are six degrees of freedom for all tests.

Experiment	Description	T-test for means (two-sided) p-value	F-test for variances p-value
1	(a) Autopipette vs. (b) Glass pipette	0.011	0.732
2	(a) One secondary solution vs. (b) Multiple secondary solutions	0.048	0.07
3	(a) Stream water vs. (b) Distilled water	0.732	0.058
4	(a) In-situ temperature vs. (b) Room temperature	< 0.001	0.485

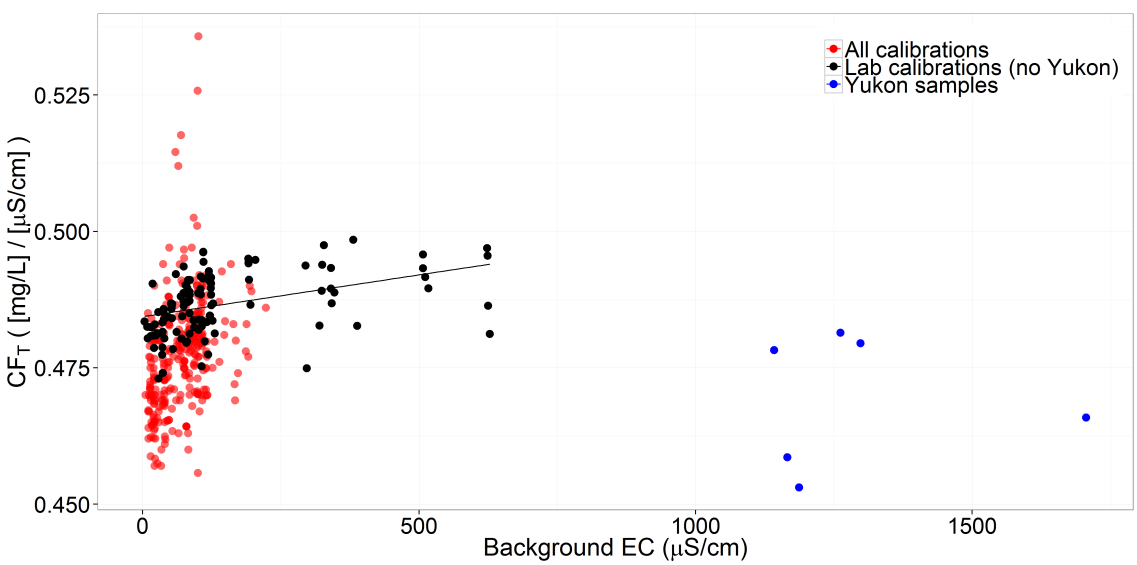

Figure 3.1: Relation between CF_T and background EC_T for salt dilution calibrations conducted in the laboratory and field. The black line is the best-fit linear relation for lab calibrations (not including the five EDI Yukon samples calibrations).

wide CF_T analysis (Experiment 5). The data points in blue are five water samples from Yukon collected by Environmental Dynamics, Inc., which display markedly different EC_{BG} and ionic composition. It is unknown how these Yukon samples were collected, or where they were collected in the province. These five Yukon samples will be referred to as the "EDI Yukon" samples. The red data points are calibrations that were performed by NHC field technicians in the past three years. The "all calibrations" and "lab calibrations without Yukon samples" both exhibit a significant positive relation between EC_{BG} and CF_T. The EDI Yukon water samples had CF_T values that deviated from the relation between CF_T and EC_{BG} for the British Columbia and other Yukon samples, plotting substantially below the best-fit line.

The Ministry of Environment Analytical Laboratory results are displayed in Table 3.3. The EDI Yukon samples and the Eagle River sample contained markedly higher concentrations of several cations, particularly boron and calcium, and one anion, sulfate. The EDI Yukon samples and the Duke River sample contained high concentrations of potassium.

Table 3.3: Cation and anion analyses results for selected water samples

Sample ID	**B** mg/L	**Ca** mg/L	**K** mg/L	**Mg** mg/L	**Na** mg/L	**P** mg/L	**F** mg/L	**Cl** mg/L	**NO_2** mg/L	**Br** mg/L	**NO_3** mg/L	**PO_4** mg/L	**SO_4** mg/L
Indian River	0.025	42.62	1.57	12.94	4.94	0.02	< 0.01	0.53	< 0.01	< 0.01	< 0.01	< 0.01	241.00
Porc Border	0.032	38.97	0.38	19.82	1.25	< 0.01	< 0.01	0.41	< 0.01	< 0.01	< 0.01	< 0.01	93.50
Duke River	0.107	77.10	3.11	16.94	6.35	< 0.01	< 0.01	0.59	< 0.01	< 0.01	< 0.01	< 0.01	157.00
Bridge South Creek	< 0.002	2.84	0.46	0.18	0.25	< 0.01	< 0.01	0.28	< 0.01	< 0.01	< 0.01	< 0.01	1.14
Bridge West Creek	< 0.002	1.24	0.24	0.19	0.36	< 0.01	< 0.01	0.28	< 0.01	< 0.01	< 0.01	< 0.01	0.36
Eagle River	0.083	77.65	0.79	25.80	16.52	< 0.01	< 0.01	0.65	< 0.01	< 0.01	1.00	< 0.01	347.00
St. Mary's Creek	< 0.002	13.77	1.02	3.58	2.40	< 0.01	< 0.01	1.17	< 0.01	< 0.01	1.29	< 0.01	14.14
Duck River	< 0.002	24.30	1.16	10.70	0.88	< 0.01	< 0.01	0.43	< 0.01	< 0.01	< 0.01	< 0.01	7.95
EDI Yukon sample #2	0.341	400.35	6.39	61.34	34.94	< 0.01	< 0.01	0.97	< 0.01	< 0.01	< 0.01	< 0.01	920.60
EDI Yukon sample #4	0.315	270.55	12.71	43.48	16.45	< 0.01	< 0.01	0.65	< 0.01	< 0.01	< 0.01	< 0.01	691.00
Tamihi West Trib	< 0.002	3.03	0.58	0.72	0.84	0.01	< 0.01	0.58	< 0.01	< 0.01	1.06	< 0.01	2.72
Gallant Creek	< 0.002	9.53	0.78	1.46	7.40	0.02	< 0.01	7.39	< 0.01	< 0.01	< 0.01	< 0.01	36.23

The water samples that were calibrated with three probes concurrently are displayed in Figure 3.2. Testing for main effects (difference in intercept), the intercepts are not significantly different from each other. Testing for main effects and interaction (difference in intercept and slope), the intercepts and slopes are not significantly different from each other (Table 3.4).

Table 3.4: Multiple linear regression for CF_T vs. EC_{BG} for triple calibrations

Main effects assuming a common slope	Estimate	Std. Error	T statistic	p-value
Intercept (WTW Black)	4.90E-01	1.15E-03	426.621	<2e-16
Slope	8.20E-06	3.17E-06	2.591	0.0135
Intercept (WTW Green)	-2.36E-04	1.36E-03	-0.174	0.8632
Intercept (WTW Red 2)	-2.52E-03	1.36E-03	-1.855	0.0714
Main effects and interaction	**Estimate**	**Std. Error**	**T statistic**	**p-value**
Intercept (WTW Black)	4.90E-01	1.48E-03	330.67	<2e-16
Slope (WTW Black)	9.34E-06	5.59E-06	1.67	0.104
Intercept (WTW Green)	-4.63E-04	2.09E-03	-0.221	0.826
Intercept (WTW Red 2)	-1.62E-03	2.09E-03	-0.773	0.444
Slope (WTW Green)	1.15E-06	7.92E-06	0.145	0.886
Slope (WTW Red 2)	-4.52E-06	7.89E-06	-0.573	0.571

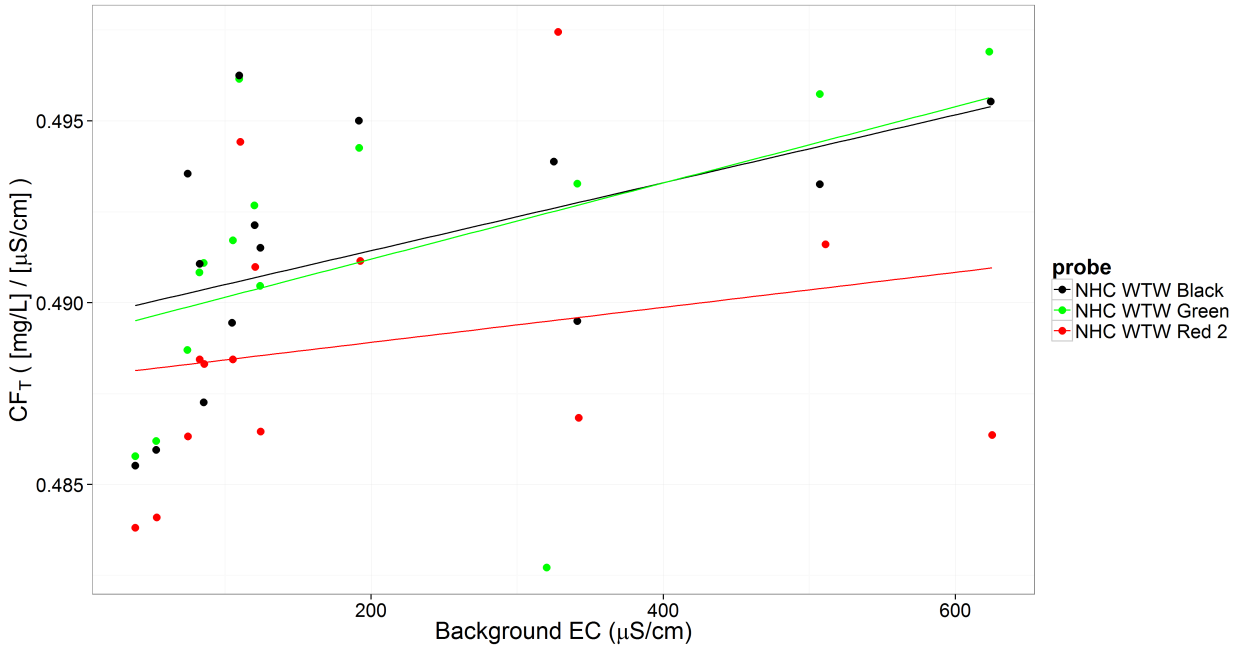

Figure 3.2: Relation between CF_T and background EC_T for salt dilution calibrations conducted with three probes concurrently. Solid lines are linear regression relations for each probe.

3.2 Mixing characteristics

Table 3.5 displays channel characteristics, discharges, and mixing lengths for different stream reaches. "Mixing length from same-side probes" indicates that two measurement probes on the same side of the stream measured similar discharges, while "mixing length from opposite-side probes" indicates that two measurement probes on opposite sides of the stream measured similar discharges. "NA" indicates that there were probes on only one side of the stream. Note that some streams have different mixing lengths based on discharge.

The mixing lengths summarized in Table 3.5 range from 2.5 to ∼25 wetted widths. However, the lack of a clear relation between discharge and stage for Bridge Glacier West Creek (Figure 3.3) suggests that the tracer was not sufficiently mixed at the measurement location to yield accurate discharge measurements. For Rutherford Creek reach 1, there was a lack of agreement between the two probes, indicating that the mixing length was at least as long as the distance between the injection point and the downstream probe.

Table 3.6 summarizes results from a reach-length case study of Carnation Creek Trib C. In all six experiments, the calculated discharge steadily increased as a function of reach length, particularly downstream of probe 4. The relative increase in discharge decreased with increasing flow levels.

3.3 Measurement location and discharge variability

Five streams were studied specifically for discharge variability in relation to probe location (Table 3.7, Figure 3.4). A measure of the uncertainty related to probe location, ε_Q, was computed as follows:

$$\varepsilon_Q = \frac{Q_{max} - Q_{min}}{0.5 \cdot (Q_{max} + Q_{min})} \tag{3.1}$$

where Q_{max} and Q_{min} are the maximum and minimum discharges among probes, respectively. Some probes were placed in areas of significant upstream flow in a side pool (Carnation Creek Trib C), in areas of turbulent whitewater (Mosquito Creek), in near-stagnant pools behind boulders (Pemberton

Table 3.5: Mixing lengths determined from discharge measurements at multiple locations

Creek	Reach	Reach slope (%)	Reach width (m)	Discharge (m^3/s)	Mixing length from same-side probes (m)	Mixing length from opposite-side probes (m)	Length/width ratio (m/m)
Bridge South Creek	1	5.7	6-8	0.818-0.859	57.1	NA	9.5
Bridge South Creek	2	7.5	6-8	0.778-0.822	14.2	NA	2.4
Bridge South Creek	3	7	6-8	1.20-1.21	147.1	NA	24.5
Bridge West Creek	1	9.5	10-12	4.58-5.44	146.5	NA	14.7
Carnation Creek Trib C	1	1.9	1.5	0.0096-0.0549	35.9	35.9	23.9
Carnation Creek Trib C	1	1.9	3.9	0.146-0.188	74.3	74.3	19.1
Carnation Creek Trib L	1	8.6	1.5	0.0087-0.0095	29.6	29.6	19.7
Pemberton Creek	1	4.1	9-11	1.26-2.28	58.3	58.3	6.5
Pemberton Creek	1	4.1	9-11	2.28-3.29	78	78	8.7
Pemberton Creek	1	4.1	9-11	3.30-3.93	107.9	NA	12
Place Creek	1	17.7	7.1	0.523-1.04	45.8	45.8	6.5
Rutherford Creek	1	4.8	12.0	2.56-3.04*	> 105*	> 105	> 8.8*
Rutherford Creek	1	4.8	12.0	4.38-5.14*	> 127.1*	> 127.1	> 10.6*
Rutherford Creek	2	3.4	7.7	1.97-3.04	142	142	18.4

* indicates well-mixed reach length was not established from multiple probe agreement

Table 3.6: Discharge measurements (m^3/s) for Carnation Creek Trib C. Reach length (m) for each probe is in parentheses. From visual field observation, the wetted width was between 1.5 m and 2.0 m for Injections 1 through 5, and unknown for Injection 6.

Injection	Probe 1 (34.9)	Probe 2 (36.9)	Probe 3 (49.2)	Probe 4 (90.7)	Probe 5 (120.2)	Probe 6 (133.2)	Probe 7 (153.7)
1	0.01	0.012	0.01	0.014	0.025	0.029	0.034
2	0.011	0.017	0.011	0.022	0.041	0.048	0.057
3	0.022	0.026	0.021	0.025	0.029	0.032	0.033
4	0.04	0.046	0.042	0.041	0.053	0.056	0.061
5	0.052	0.057	0.053	0.052	0.063	0.068	0.071
6	NA	NA	NA	0.735	0.768	0.809	0.865

Creek), or in fast-flowing narrow chutes of water (Pemberton Creek). Despite obvious differences in BTC shape (Figure 3.4), all measured discharges were in reasonable agreement for each injection ($< \pm 10$ %).

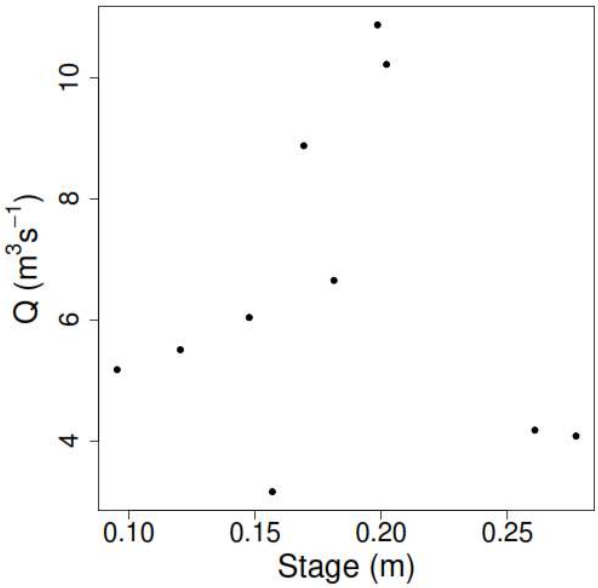

Figure 3.3: Stage-discharge relation for Bridge Glacier West Creek (data from Moyer, 2015). Rating curve and errors bands are not provided due to lack of relation between stage and discharge.

Table 3.7: Discharge measurements for injections focusing on measurement location variability. The value of ε_Q is a measure of the percent error in measured discharge for one injection.

Stream	Injection	Number of probes	$0.5 \cdot (Q_{max} + Q_{min})$ (m^3/s)	Q_{max} - Q_{min} (m^3/s)	ε_Q ($\pm$%)	Notes on probe location
Carnation Trib C	1	3	0.0109	0.0016	7.1	narrow stream (w = 2 m)
	2	3	0.0238	0.0045	9.5	narrow stream (w = 2 m)
	3	3	0.0400	0.0035	4.4	narrow stream (w = 2 m)
	4	3	0.0515	0.0074	7.2	narrow stream (w = 2 m)
Carnation Trib L	1	3	0.0094	0.0006	3.1	narrow stream (w = 1.5 m)
	2	3	0.0090	0.0008	4.3	narrow stream (w = 1.5 m)
Mosquito Creek	1	5	0.349	0.020	2.9	distributed across stream channel
	2	5	0.267	0.009	1.8	distributed across stream channel
	3	5	0.303	0.032	5.3	distributed across stream channel
Pemberton Creek	1	2	2.24	0.07	1.5	both sides of stream
	2	3	2.30	0.18	3.9	both sides of stream
	3	3	2.17	0.13	3.0	both sides of stream
	4	3	2.16	0.16	3.6	both sides of stream
	5	3	2.14	0.11	2.7	both sides of stream
	6	3	2.19	0.23	5.4	both sides of stream
	7	3	2.09	0.08	1.8	both sides of stream
	8	3	2.04	0.34	8.4	both sides of stream

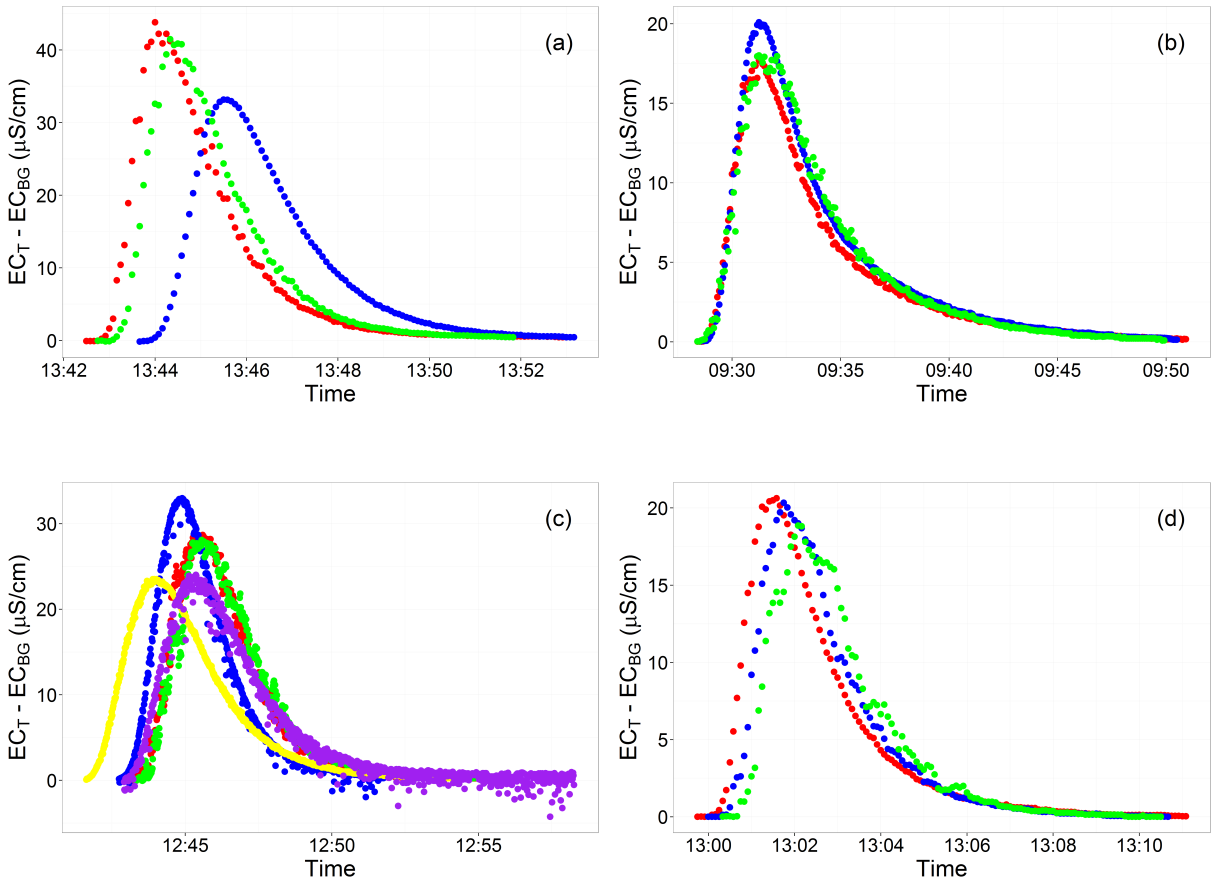

Figure 3.4: BTCs for discharge measurements focused on measurement location variability. One sample injection for each stream. Different colours are the BTCs for different probes for the same injection: (a) Carnation Creek Trib C Injection 3 (Q = 0.040 $m^3/s \pm 4.4\%$; (b) Carnation Creek Trib L Injection 2 (Q = 0.0090 $m^3/s \pm 4.3\%$; (c) Mosquito Creek Injection 1 (Q = 0.349 $m^3/s \pm 2.9\%$; (d) Pemberton Creek Injection 5 (Q = 2.14 $m^3/s \pm$ 2.7%.

3.4 Dosage guidelines: relations between A^* and reach characteristics

Values of A^* ranged from 0.25 to 0.93, with an average value of 0.55 (Figures 3.6 and 3.7). The spread of A^* values is less for the field study streams compared to the NHC streams, although the average values are similar. The spread of A^* values decreases when looking at specific streams. Carnation Creek Trib L had high A^* values relative to all other streams. Based on the nondimensional BTCs (Figure 3.5), there are two observed trends: (1) the tails of the non-dimensional BTCs were longer (or "shallower") for larger A^* values; and (2) the non-dimensional first arrival times (τ_0) were earlier for larger A^* values.

When looking at all streams, there is a positive trend between A^* values and discharge (Figure 3.8), and a negative trend between A^* and reach length (Figure 3.9). The Pemberton Creek measurements for a long reach length (x_m = 53·w, seen as outlier dots on Figure 3.6) had much lower A^* values than compared to the other Pemberton Creek measurements.

A series of measurements at Pemberton Creek were taken for a wide range of discharges at a constant reach length (Figure 3.10). A weak positive relation was observed between A^* and discharge (p = 0.053). A series of measurements at Carnation Creek Trib C were taken at different reach lengths for a constant discharge (Figure 3.11). The spread of these A^* values is low, although there is a significant negative relation between A^* and reach length ($p < 0.001$), as was also observed for the long reach length experiments at Pemberton Creek.

Table 3.8 shows variability of A^* based on measurement location. Carnation Creek Trib L had similar A^* values for all three probes, and the stream was significantly narrower than the other streams (wetted width = 1 m). The highest and lowest A^* values occurred in all areas of the stream (e.g. slow side-pool, main water column), indicating that there is no systematic relation between A^* value and measurement location across different streams. However, for each stream, the highest and lowest values of A^* occurred at the same measurement location for all injections, indicating that the measurement location variability is dependent on the stream but consistent between different injections.

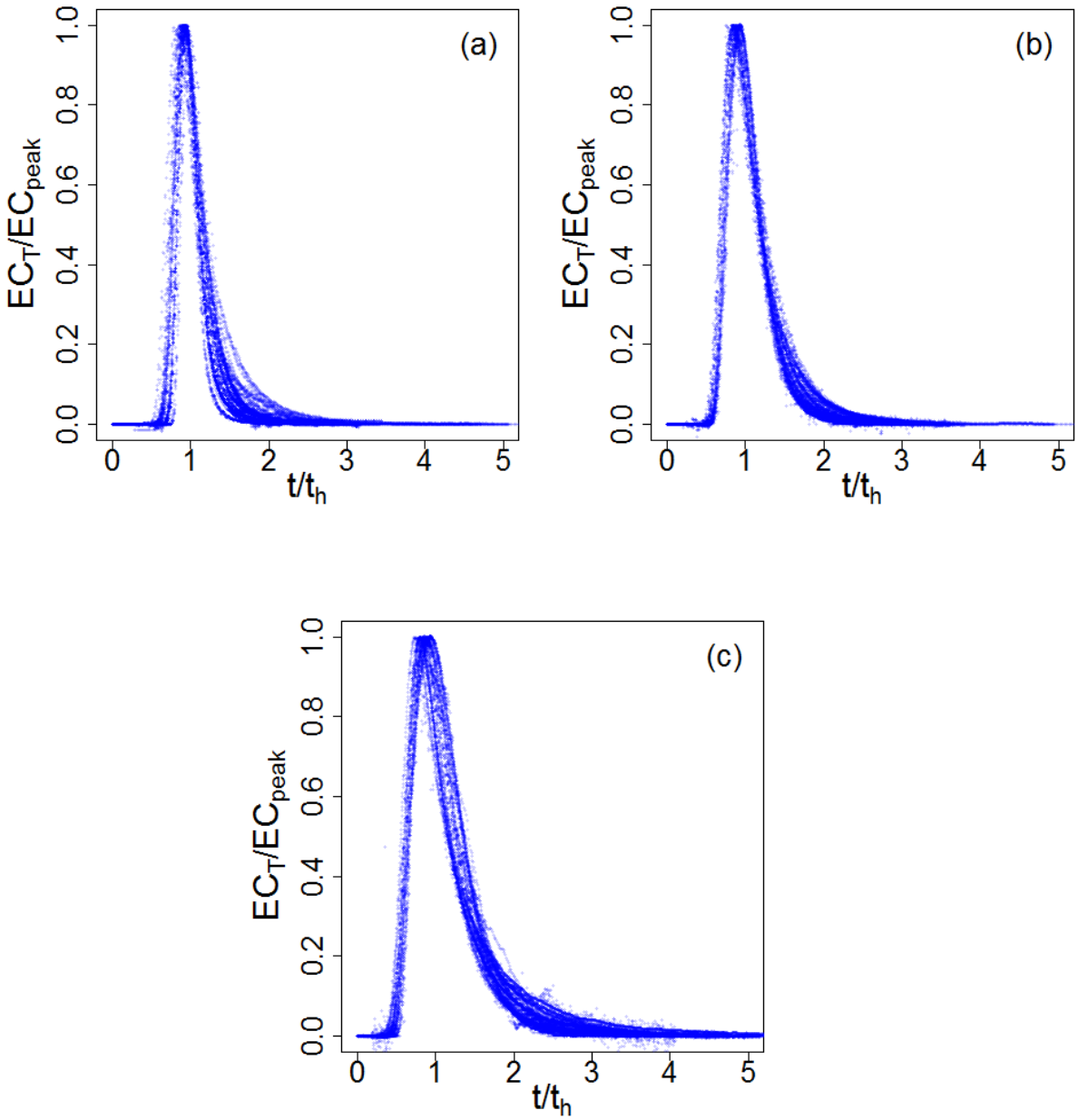

Figure 3.5: Plots of all non-dimensional BTCs: (a) BTCs with A^* values between 0.24 and 0.49 (n = 51), (b) BTCs with A^* values between 0.49 and 0.62 (n = 67), and (c) BTCs with A^* values between 0.62 and 0.94 (n = 51).

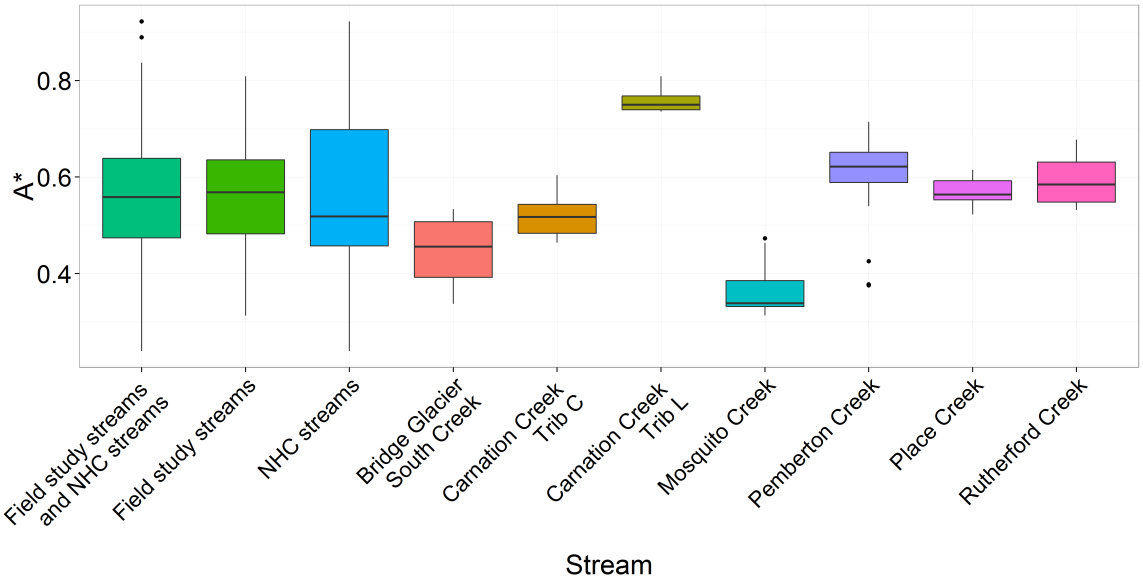

Figure 3.6: Boxplot of A^* values for all injections (field study streams and NHC streams) and for each field study stream.

Table 3.8: Measurement location variability of A^*. Highest/lowest A^* is the highest/lowest average A^* value from one probe for all injections at that stream. In the location description, the value in brackets is a visual estimate of the ratio of the local velocity near the probe to the maximum local velocity across the channel.

Stream	Number of probes	Highest A^*	Lowest A^*	Location description of highest A^*	Location description of lowest A^*
Bridge Glacier West Creek	4	0.45	0.36	Fast flowing water [speed 4/5]	Directly underneath water chute [speed 3/5]
Carnation Creek Trib L	3	0.77	0.75	Slow pool [speed 1/5]	Directly underneath water chute (speed 3/5)
Mosquito Creek	5	0.46	0.32	Fast flowing water [speed 4/5]	Steady flow in main water column [speed 3/5]
Pemberton Creek	3	0.64	0.59	Steady flow in main water column [speed 3/5]	Slow side-pool [speed 1/5]

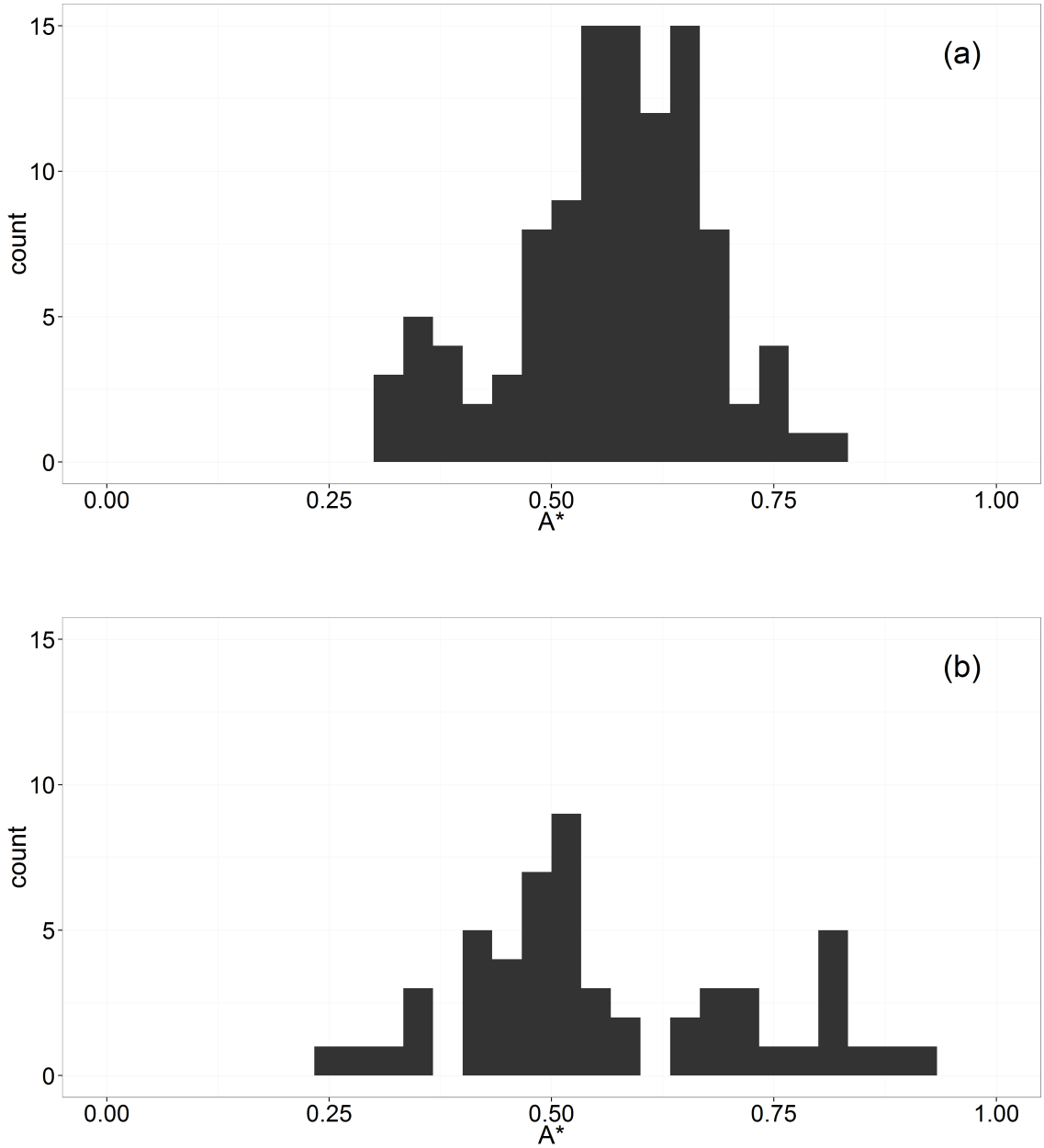

Figure 3.7: Histograms of A^* values: (a) Field study streams (n = 121); (b) NHC streams (n = 54).

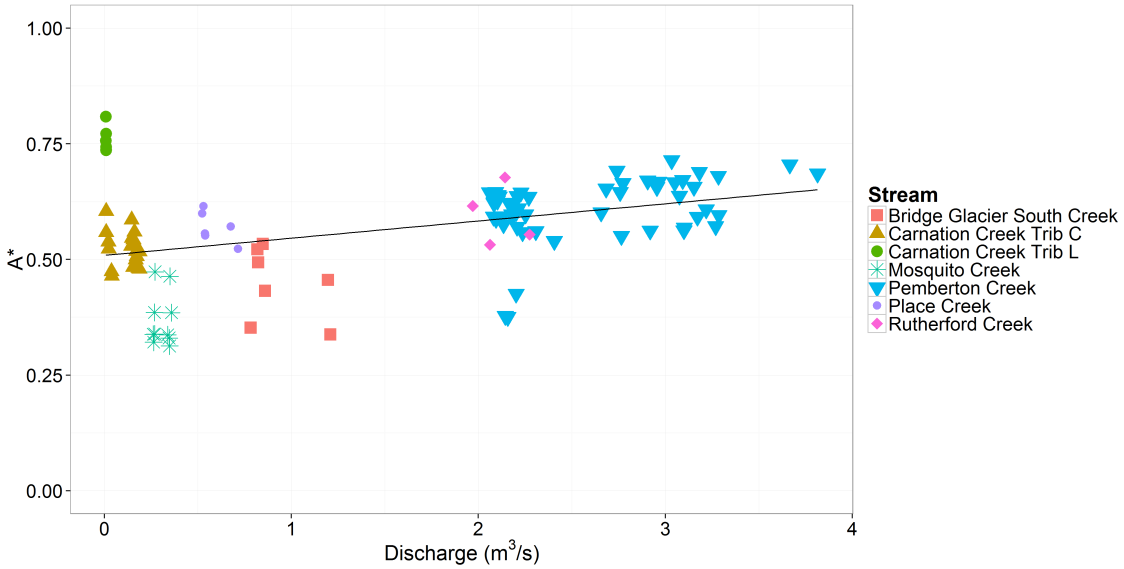

Figure 3.8: Variability of A^* with discharge, for all injections from all field study streams (n = 121). The black line is a linear regression fit to provide visual reference.

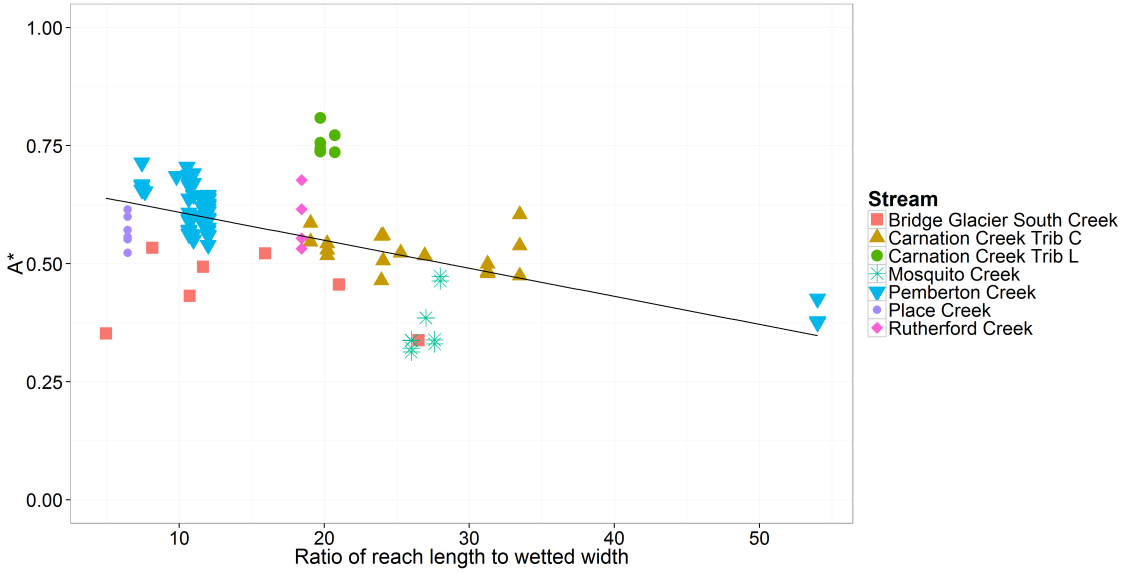

Figure 3.9: Variability of A^* with ratio of reach length to wetted width, for all injections from all field study streams (n = 121). The black line is a linear regression fit to provide visual reference.

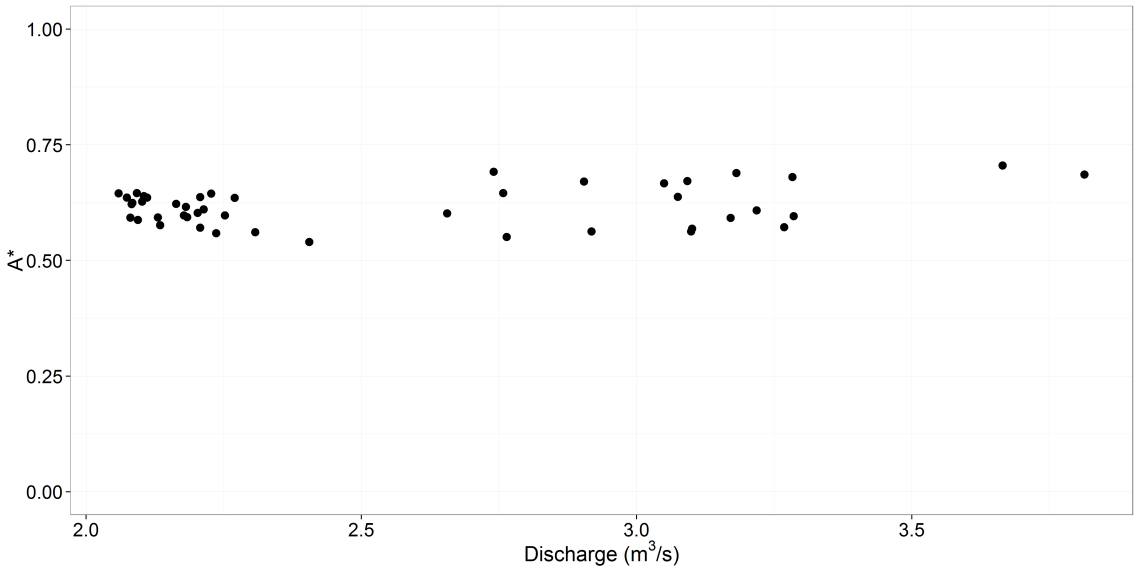

Figure 3.10: Variability of A^* with discharge, for a constant reach length, at Pemberton Creek. There was no significant linear relation found.

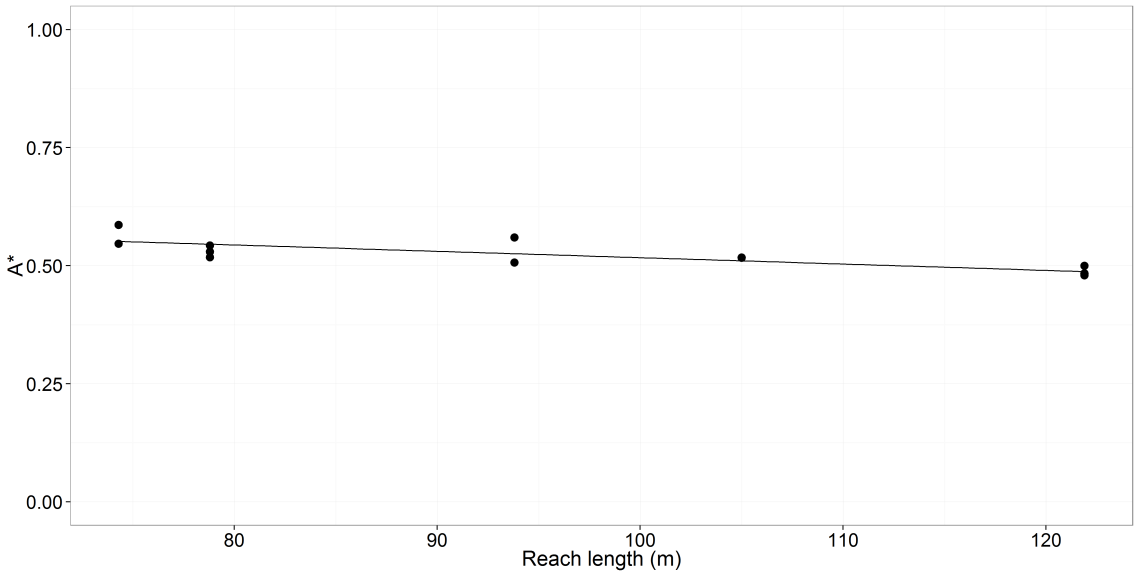

Figure 3.11: Variability of A^* with reach length, for constant discharge, at Carnation Creek Trib C. Black line is linear regression relation for all injections ($p < 0.001$).

3.5 Rhodamine WT dilution gauging

3.5.1 Laboratory calibrations and experiment for Rhodamine WT

Summaries of the means, standard deviations, and coefficients of variation for each calibration condition are provided in Table 3.9. As shown in Table 3.10, there were no significant differences in CF_R variance between probes or between turbidity levels. The probe used did not have a significant effect on CF_R value, but the level of turbidity did have a significant effect.

Table 3.9: Results for each set (n = 7) of Rhodamine WT calibrations

Probe	Turbidity	Mean CF_R [(g/L)] / mV]	Standard deviation of CF_R [(g/L)] / mV]	Coefficient of Variation
WSC_A	low	6.82E-05	0.30E-05	4.3%
WSC_A	high	7.48E-05	0.35E-05	4.6%
WSC_B	low	6.71E-05	0.22E-05	3.3%
WSC_B	high	7.58E-05	0.30E-05	4.0%

Table 3.10: Statistical tests for comparisons between turbidity levels and between probes for Rhodamine WT calibrations

F-tests for variances (6 degrees of freedom for each test)			
Turbidity level	Probe	p-value	
Low vs. high turbidity	WSC_A	0.49	
Low vs. high turbidity	WSC_B	0.72	
Low turbidity	WSC_A vs. WSC_B	0.69	
High turbidity	WSC_A vs. WSC_B	0.46	
Two factor analysis of variance			
Factor	Degrees of freedom	F-value	p-value
Probe (WSC_A and WSC_B)	1	0.165	0.688
Turbidity (low and high)	1	53.7	< 0.001
Residuals	25		

Figure 3.12 shows results from the full laboratory experiment. Both RWT probes exhibited similar behavior, and only one probe's data are presented here. RWT and turbidity measurements

were averaged over 60-s intervals for visual clarity. The background fluorescence of the sample stream water was approximately 67 mV.

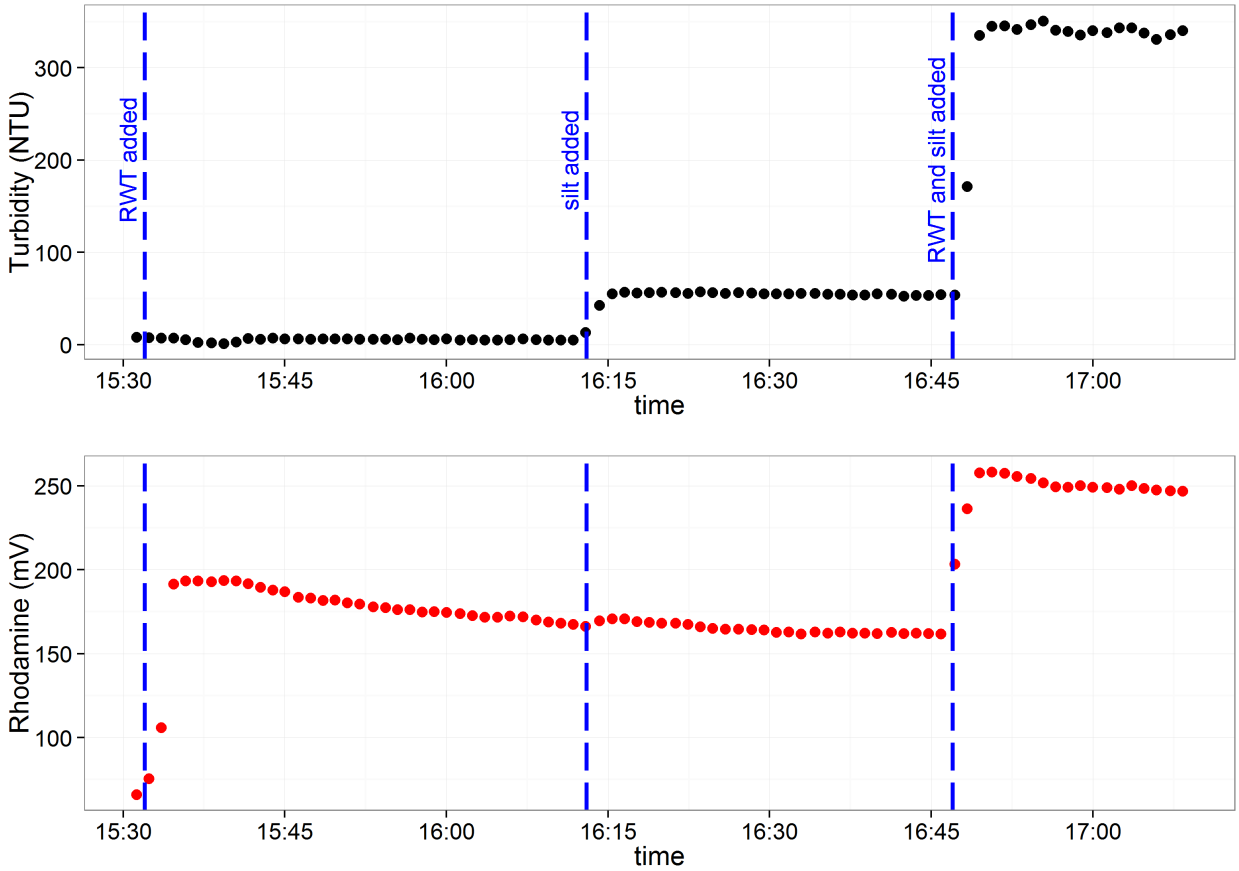

Figure 3.12: Time series plots of turbidity (top) and Rhodamine WT (bottom) for laboratory experiment. Blue vertical lines indicate addition of RWT and/or silt to the water sample.

Figure 3.13 highlights three 15-min intervals of the full experiment. RWT concentration was measured at 1-s intervals. Over the 15 minutes, approximately 10%, 5%, and 5% of the RWT was lost due to decay for the no silt, low silt, and high silt measurements, respectively. Although the high silt content and no silt content trials had similar decay rates, the initial RWT concentration during the high silt content measurements was double the initial RWT concentration during the no silt content measurement, resulting in half the proportional decay rate. It was observed during the experiment that the measurements became noisier at higher suspended sediment concentrations.

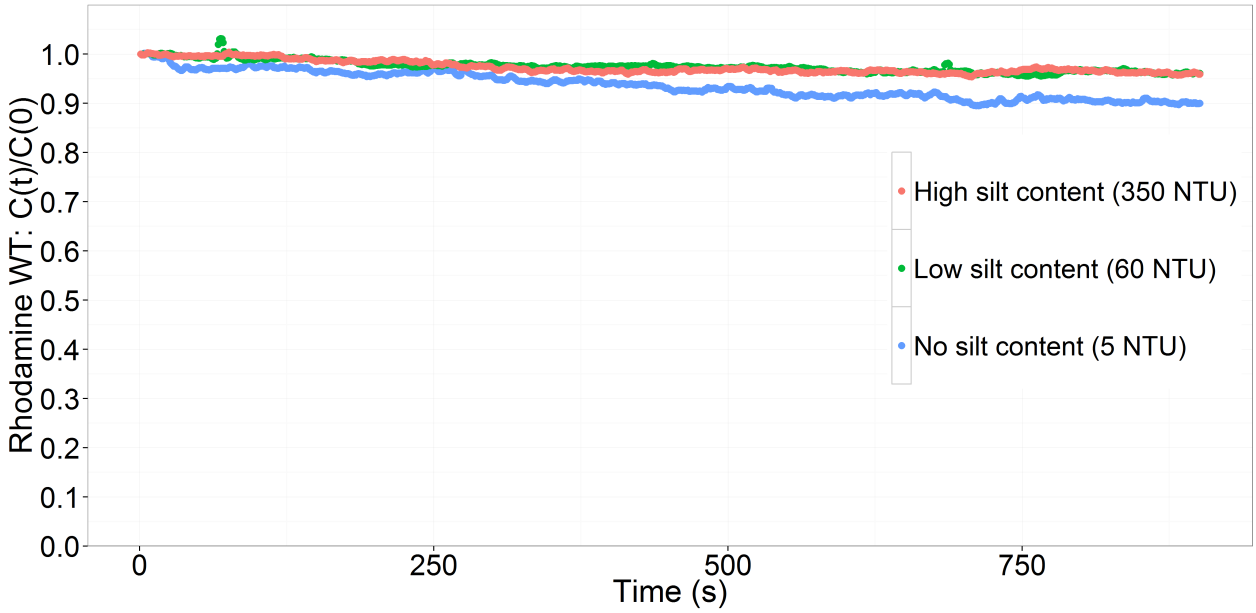

Figure 3.13: Rhodamine WT decay at different silt concentrations. The y axis shows the ratio of RWT concentration to the initial concentration.

3.5.2 Stream gauging with Rhodamine WT

Calibrations of the stream water for all eight probes (four RWT, four salt) were performed off-site in a laboratory setting. Despite using the same calibration approach as discussed in Section 2.3.2, the RWT calibrations were not consistent (Table 3.11). Different CF_R values were obtained for multiple calibrations of the same probe. For Hoskin$_B$, WSC$_A$, WSC$_B$, the average of two calibration CF_R values were used for calculating discharge. For Hoskin$_A$, the CF_R value of the first calibration was used due to its similarity to Hoskin$_B$ CF_R values and due to similar peak/background ratios during the gaugings.

Table 3.12 shows signal:noise observations for the RWT discharge measurements. The Hoskin probes (downstream) behaved in a similar fashion, while the WSC probes (upstream) did not.

Discharge measurement results are shown in Table 3.13. Measurement uncertainties were determined as per the method described in Section 2.4.1. CF_R uncertainty was taken as the difference of the two measured CF_R values divided by two. The relatively high uncertainty associated with the Rhodamine WT discharge measurements are due to (1) CF_R uncertainty for all measurements, and

Table 3.11: CF_R values used for field discharge measurements

Probe	Calibration	CF_R	CF_R used for measurement	r^2	Number of calibration points
$Hoskin_A$	1	0.56E-4	0.56E-4	0.999	3
	2	1.46E-4		0.978	7
$Hoskin_B$	1	0.45E-4	0.41E-4	0.937	6
	2	0.37E-4		0.998	6
WSC_A	1	1.07E-4	1.21E-4	0.977	8
	2	1.34E-4		0.998	5
WSC_B	1	1.25E-4	1.36E-4	0.991	6
	2	1.46E-4		0.986	6

Table 3.12: Signal/noise observations for the RWT discharge measurements

Probe	Location	Injection	Mass injected (g)	Background uncertainty (± mV)	Peak:background ratio (mV:mV)
WSC_A	Upstream	1	1.4893	0.3	150:85
		2	2.1439	0.3	190:85
		3	1.9986	0.3	185:85
WSC_B	Upstream	1	1.4893	0.7	135:100
		2	2.1439	0.7	155:95
		3	1.9986	0.7	150:95
$Hoskin_A$	Downstream	1	1.4893	1.5	220:120
		2	2.1439	1.5	290:120
		3	1.9986	1.5	280:120
$Hoskin_B$	Downstream	1	1.4893	1.5	225:125
		2	2.1439	1.5	280:125
		3	1.9986	1.5	275:125

(2) an unstable background RWT measurement in relation to the peak to background ratio for some measurements and probes (Tables 3.12 and 3.13). The WSC_B and $Hoskin_A$ probes consistently measured markedly different discharges than the other six probes (even if they were within tolerance bounds for measurement agreement for some injections).

Table 3.13: Discharge measurements for RWT and salt dilution gauging at Mosquito Creek, North Vancouver, BC

Injection	Probe	Type	Location	Discharge (m^3/s)	Discharge uncertainty (%)	Measurement agreement? (with WTW_{red} and WTW_{yellow})
1	WTW_{red}	Salt	Upstream	1.06	9.0	Yes
	WTW_{yellow}	Salt	Upstream	1.07	4.6	Yes
	WSC_A	RWT	Upstream	1.05	15.5	Yes
	WSC_B	RWT	Upstream	1.97	43.0	Yes
	WTW_{black}	Salt	Downstream	1.13	3.4	Yes
	WTW_{green}	Salt	Downstream	1.10	6.5	Yes
	$Hoskin_A$	RWT	Downstream	0.76	37.5	Yes
	$Hoskin_B$	RWT	Downstream	1.08	30.4	Yes
2	WTW_{red}	Salt	Upstream	0.93	3.4	Yes
	WTW_{yellow}	Salt	Upstream	0.93	4.7	Yes
	WSC_A	RWT	Upstream	0.92	15.3	Yes
	WSC_B	RWT	Upstream	1.23	34.5	Yes
	WTW_{black}	Salt	Downstream	0.96	6.4	Yes
	WTW_{green}	Salt	Downstream	0.95	6.6	Yes
	$Hoskin_A$	RWT	Downstream	0.66	28.1	No
	$Hoskin_B$	RWT	Downstream	0.94	19.6	Yes
3	WTW_{red}	Salt	Upstream	0.88	3.1	Yes
	WTW_{yellow}	Salt	Upstream	0.88	3.1	Yes
	WSC_A	RWT	Upstream	0.88	13.5	Yes
	WSC_B	RWT	Upstream	1.43	15.2	No
	WTW_{black}	Salt	Downstream	0.93	5.8	Yes
	WTW_{green}	Salt	Downstream	0.92	5.9	Yes
	$Hoskin_A$	RWT	Downstream	0.63	28.3	No
	$Hoskin_B$	RWT	Downstream	0.86	20.3	Yes

Chapter 4

Discussion

4.1 Calibration factors for salt dilution via dry slug injection

4.1.1 Experiments 1 through 4

Although the mean CF_T values differed significantly between methods for Experiment 1, the difference is small (0.5%) and of the same order of magnitude as the uncertainty associated with the equipment used for calibration. The variances are similar between methods. These results indicate that using an autopipette versus a glass pipette has little effect on the uncertainty of the calibration, and ultimately the choice in equipment should be based on user preference.

As was the case for Experiment 1, the differences in mean CF_T values between methods for Experiment 2 are statistically significant (at $\alpha = 0.05$) but small (0.3%). The variance in CF_T of using a new secondary solution for each calibration is smaller than using one secondary solution for all calibrations. These results suggest that mixing a new secondary solution for each calibration will minimize CF_T variability. However, if time constraints do not allow mixing a new solution for each calibration, the resulting error should be under 1% based on the experimental results.

In Experiment 3, there was no significant difference among CF_T values, which suggests that the distilled water correction (Equation 2.5) adequately accounts for the differences in ionic composition of the stream water and distilled water. However, the background EC_T of the stream water

was low (37 $\mu S \cdot cm^{-1}$), and thus the correction was minor. More calibration tests for Experiment 3 should be performed with high EC_{BG} stream water, as the correction would have a larger influence on the derived CF_T.

The variance of using distilled water for the calibration solution is smaller than using stream water for the calibration solution. These results suggest that using distilled water for the secondary solution will minimize CF_T variability. However, the errors from using distilled water or stream water for the secondary solution should both be under 1% based on the experimental results, as long as the distilled-water correction is applied. Therefore, the choice in secondary solution solvent should be based on user preference.

For Experiment 4, the 1.3 % difference in mean CF_T values between the methods is statistically significant. This difference is likely due to inaccuracies of the nonlinear correction applied to the electrical conductivity based on temperature. The correction method is known to be most inaccurate as the water temperature drops below 3 °C and approaches 0 °C (Moore et al., 2008). Therefore, the calibration procedure should be performed at in-situ water temperature when possible. In the field, the calibration container should rest directly in the stream to ensure the temperature is similar to that of stream water, as recommended by Moore (2005).

4.1.2 Experiment 5 - province-wide CF_T analysis

Although the regressions are significant, the relative change in CF_T is small over a large range of EC_{BG}. For example, the CF_T changes by approximately 1.5% over a range of 500 μS/cm for the lab calibrations. Theoretically, higher concentrations of ions impede their mobility, resulting in a weaker positive relation between EC and concentration as more ions are present in the solution (Hem, 1982; Moore et al., 2008). Therefore, one would expect an increase in CF_T with an increase in EC (and EC_T), which agrees with calibrations in this study (disregarding the EDI Yukon samples).

The value of CF_T will vary depending on the chemical species present in the stream water (Hem, 1982; Moore et al., 2008). Therefore, one would expect different values of CF_T depending on the relative proportions of different ions in the water. The low CF_T values of the EDI Yukon samples

may be due to significantly higher concentrations of several cations (boron, calcium, and potassium) and/or one anion (sulfate). However, water from Eagle River in Yukon, with a relatively high EC_{BG}, also contained high concentrations of many of these ions without exhibiting a characteristically low CF_T. Potassium (K) was not present in Eagle River water in notable quantities, but was present in high concentrations in the EDI Yukon water samples. The Duke River water, also from Yukon, contained high concentrations of potassium, but its CF_T was not markedly low in comparison to other water samples' CF_T values. The relatively large concentration of potassium ions could be affecting the calibrations of the EDI Yukon samples, but there is not enough information to draw firm conclusions.

For the triple calibrations, the differences among probes are statistically insignificant. The three probes had very similar calibration constants (0.469, 0.470 and 0.469 for Red, Green and Blue, respectively). The "NHC WTW Red 2" (Red) probe produced systematically lower CF_T values than the other two probes. Based on the linear regressions, the Red probe produced CF_T values that were approximately 0.4% to 1.0% lower. At least among similar devices, this study shows that one should expect similar CF_T values, assuming the probes are properly calibrated. However, given the systematic difference shown by the Red probe, and that there are many electrical conductivity meters available for use, one should always use the same device to measure the discharge and calibrate the stream water. It would be beneficial to replicate these concurrent calibrations with more devices (especially non-WTW devices).

4.1.3 Guidelines for determining CF_T uncertainty

As discussed in Section 2.4.1, δ_{CF_T} should vary based on the calibration conditions for each dilution measurement. Table 4.1 presents a framework to determine the value of δ_{CF_T}. Adequate calibration conditions would involve an experienced user, fair weather conditions, adequate equipment (glassware, properly calibrated EC_T measurement probe, etc.), and calibrating at in-situ stream temperature. Non-adequate conditions could involve an inexperienced user, wet weather conditions (e.g. if rainwater is splashing into the calibration container, diluting the salt concentration), non-adequate

equipment (plasticware, damaged equipment, etc.), and calibrating at air temperature. Extra care should be taken to calibrate stream waters with very high EC_{BG} values, as the EDI Yukon samples calibrated in this study had the highest EC_{BG} values and did not follow the same trends observed from the other stream water samples.

Table 4.1: Values of δ_{CF_T} for different calibration conditions, using an example CF_T value of 0.48 $\mathrm{L \cdot cm \cdot \mu S^{-1} \cdot m^{-3}}$. The value of SD is the standard deviation of the calibrations performed in Experiment 1(a), the value of SE_{all} is the residual standard error of the linear relation between CF_T and EC_{BG} for all calibrations (from this study and from NHC field calibrations), and the value of SE_{lab} is the residual standard error of the linear relation between CF_T and EC_{BG} for the laboratory calibrations from Experiment 5 (disregarding the EDI Yukon water samples' CF_T values).

Calibration condition	Uncertainty method	Value used in δ_{CF_T} determination ($\mathrm{L \cdot cm \cdot \mu S^{-1} \cdot m^{-3}}$)	δ_{CF_T} for CF_T = 0.48 $\mathrm{L \cdot cm \cdot \mu S^{-1} \cdot m^{-3}}$
Calibration performed in adequate conditions	Based on repeatability of calibration. $\delta_{CF_T} = 2 \cdot SD$	SD = 0.001604	0.7%
Calibration performed in non-adequate conditions	Based on variability of CF_T values from all available calibration data (n = 434). $\delta_{CF_T} = 2 \cdot SE_{all}$	SE_{all} = 0.009746	4.1%
CF_T is estimated, no calibration performed	Based on relation between CF_T and EC_{BG} from Experiment 5 (n = 116). $\delta_{CF_T} = 2 \cdot SE_{lab}$	SE_{lab} = 0.005037	2.1%

4.2 Mixing characteristics

Day (1977) found that using a reach length x_m equal to or exceeding 25 wetted widths (w) was sufficient for complete tracer mixing from 41 dilution gaugings across five mountain streams. He found that the typical minimum adequate mixing length ranged from $x_m = 8 \cdot w$ to $x_m = 25 \cdot w$. With the exception of Bridge South Creek Reach 2, the mixing lengths in this study generally agreed with Day (1977), with x_m ranging between $6.5 \cdot w$ and $24.5 \cdot w$. In both studies, it is apparent that mixing lengths are reach-dependent as expected.

In this study, it was observed that it can be problematic to use two probes on the same side of the stream to confirm adequate mixing. The experiments at Rutherford Creek Reach 1 had same-side

probe agreement, but disagreement in the opposite-side probe measurement. Two probes on the same side of the injection location yielded a discharge of 2.60 ± 0.05 m^3/s, while one probe on the opposite side of the injection location measured a discharge of 20.9 m^3/s. This extreme discrepancy was seen during all injections, and all probes were approximately the same distance downstream of the injection point ($x_m = 104 \pm 1$ m). Using only the same-side probes, this measurement would be taken as adequate, when it is obvious that complete mixing has not occurred across the entire stream channel. Another example of this "same-side error" was seen at Bridge Glacier West Creek. The discharges yielded from the four probes were in agreement, but there was a poor relation between stage and discharge (Figure 3.3), indicating that the measurements were not accurate, likely due to incomplete mixing across the stream channel.

This "same-side error" may confound any of the results in Table 3.5 that only have same-side measurement confirmation. For example, it seems highly improbable that x_m of Bridge South Creek Reach 2 is equal to 2.4 w. The same-side error suggests that (1) opposite side probes are necessary to confirm adequate mixing, and (2) at least one opposite side probe is needed to confidently study mixing lengths as in this study. Day (1977) did not comment on his methodology for measurement location.

It was observed at Carnation Creek Trib C that determining adequate mixing length and verifying discharge measurements can be confounded by stream-subsurface water fluxes. A steadily increasing discharge with increasing reach length indicates that the stream was gaining water through the reach, diluting the tracer, and causing a higher discharge measurement downstream (Table 3.6). This phenomenon has been reported by others (e.g. Zellweger et al., 1989; Clow and Fleming, 2008). The bottom portion of Trib C (location of Probe 4 and further downstream) flows across the floodplain of the main stem of Carnation Creek. Groundwater could be discharging into Trib C from Carnation Creek's floodplain aquifer. In addition, some of the injections were performed during a rain event, and surface and near-surface runoff likely entered the stream throughout the measurement reach. Clow and Fleming (2008) used constant-rate injection to confirm complete mixing, and found a steady increase in discharge moving downstream. However, they could not

distinguish whether it was due to surface-subsurface water fluxes or RWT decay.

In some scenarios, stream-subsurface water fluxes make it almost impossible to determine the correct discharge and adequate mixing length, since probes at different mixing lengths, but downstream of complete mixing, can yield different discharges. It may be most difficult to reconcile this issue in small streams, where the stream is too narrow to space two probes an adequate distance apart on opposite stream sides. For larger streams, the mixing length may be able to be reconciled more easily, as probes on the same side as the injection point generally underestimate the discharge (higher tracer concentration), while probes on the opposite side generally overestimate the discharge (lower tracer concentration), if x_m is too short. This situation was seen at Rutherford Creek Reach 1 (discussed above). In these scenarios, the discharge measurements from either stream side should converge as the probes are moved downstream, until the discharge measurements agree, and adequate mixing can be assumed.

These discussions lead to spatial considerations. It is useful to understand the water flux tendencies between the stream reach of interest and the surrounding area. For example, at Carnation Creek Trib C, it would be advisable to choose a stream reach further upstream of the Carnation Creek floodplain. Losing reaches and gaining reaches will affect the discharge measurement differently. If the stream is losing water downstream of complete mixing, it would lose equal amounts of water and tracer, with no effect on the measured discharge. However, if the stream is losing water prior to complete mixing, it would likely affect the measurement. Therefore, a losing reach would accumulate measurement error only in the mixing reach, while a gaining reach would accumulate measurement error throughout the entire measurement reach (mixing reach and downstream of the mixing reach). In both cases, it is best to measure the discharge at the minimum x_m that guarantees complete mixing to minimize the effects of lateral water fluxes (e.g. groundwater recharge and discharge).

In contrast to Trib C, a long reach length was not an issue at Pemberton Creek. Measurements at lengths $x_m = 12 \cdot w$ and $x_m = 54 \cdot w$ agreed. Lateral channel inputs of water were likely more insignificant at this stream due to the following: (1) the area was dry at the time; (2) Pemberton Creek is a

glacier-fed stream, and receives most of its water from a point source upstream, especially during dry conditions; (3) Pemberton Creek is a steeper, valley-incised stream, and is likely not influenced by the near vicinity of other streams; (4) the drainage area for Pemberton Creek is significantly larger than the drainage area for Trib L, and therefore the effect of lateral water fluxes per unit of stream length will be smaller in comparison to the total flow.

Based on the preceding reach-length discussion, the discharge measurement is dependent on the specific measurement reach. Therefore, if one is comparing discharges over time (e.g. generating a rating curve), one should try to use a given measurement reach consistently (i.e. the same injection point and measurement point for all injections). However, stream-subsurface water fluxes and the adequate mixing length will vary based on discharge, so using the same measurement reach will not completely resolve these issues.

The potential issues associated with "same-side" measurement error and stream-subsurface water fluxes may be impossible to reconcile in some situations, but being aware and knowledgeable of them will aid in attributing uncertainty levels and confidence to discharge measurements.

4.3 Measurement location and discharge variability

Under favorable conditions (e.g. steady EC_{BG}, confident calibration procedure), the uncertainty (δ_{dp} or δ_{dm}) in discharge measurement may be low ($< 5\%$). The uncertainty in Q for many of the experiments in Table 3.7 is larger than 5%. It is common to attribute a measurement discrepancy between probes to inadequate mixing (i.e. x_m is too short), but this study shows that the discrepancy can also be due to measurement location even if the tracer is well-mixed at the measurement location.

There was no discernible relation between measurement location and discharge (e.g. if all probes in fast-flowing water had closer measurement agreement than probes in slow-flowing pools). Probes that were located in fast-moving chutes of water generally had the smoothest BTCs (e.g. in Figure 3.4: Carnation Creek Trib C, blue BTC; Mosquito Creek; yellow BTC). Smooth BTCs are preferred because they indicate that the tracer is arriving at the measurement location in a continu-

ous flow of tracer material. However, a smooth BTC does not confirm that the tracer is well-mixed throughout the stream channel. For example, Figure 4.1 shows a smooth BTC from Bridge Glacier South Creek, but it is highly unlikely that complete mixing had occurred at the measurement location ($x_w = 2.4 \cdot w$).

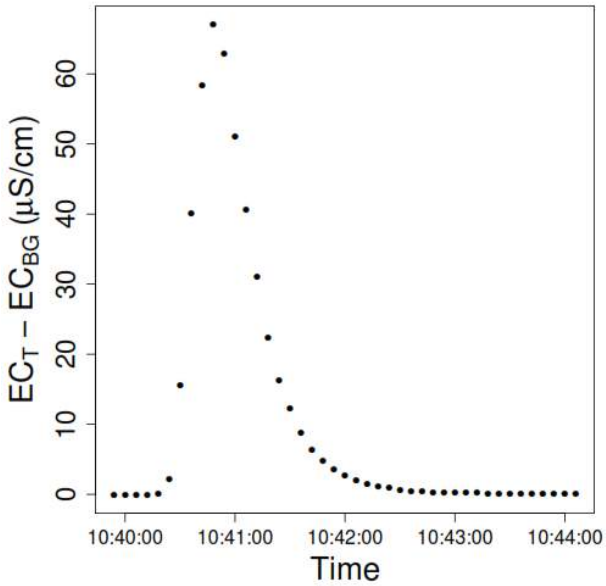

Figure 4.1: Example BTC from Bridge Glacier South Creek. Despite the smooth shape, it is highly unlikely that adequate mixing had occured across the stream channel, considering the reach length was only 2.4 wetted widths.

Abrupt changes in EC_T indicate that the tracer is arriving in discontinuous "pockets" of tracer material, which is not reflective of a well-mixed water column. Examples of choppy BTCs in Figure 3.4 that exhibit abrupt changes include the green BTC at Pemberton Creek and the green BTC at Carnation Creek Trib L. The probes that recorded choppy BTCs were generally located in areas of slow moving water (side-pools, behind obstructions). The choppiness also suggests that the stream reach is not long enough to allow for adequate mixing. In the case of Pemberton Creek, both the green BTC probe and the blue BTC probe were in slow side-pools, but the green BTC probe was on the opposite side of injection. Although the measurements agreed well in this case, the tracer was likely not completely well mixed across the entire stream channel. BTC choppiness may also be due to probe placement in areas of aerated water, as air bubbles will cause a downward spike in

EC_T reading (e.g. in Figure 3.4: Mosquito Creek, purple BTC). Moore (pers. comm.) has observed choppy BTCs in areas with groundwater discharge through the bed.

From these results, it is advised to place the measurement probes in areas of fast-flowing, non-aerated water when possible. For determining discharge, measurement location may substantially lower the precision of the measurement, even at a location downstream of complete mixing. Qualitatively, these experiments have shown that measurement location can have a significant effect on the shape of the BTC, and may confound other findings that use BTC shape to quantify residence times of solutes and transient storage parameters (e.g. Szeftel et al., 2011; Jimnez and Wohl, 2013; Gonalez-Pinzon et al., 2013). Studies using tracer dilution should always provide a photograph and detailed description of measurement location in relation to area of the channel (e.g. same/opposite side of injection, behind an obstruction), reach length, reach width, and speed of the water column (e.g. in a back-eddy, in aerated fast-flowing water).

4.4 Dosage guidelines

4.4.1 Relations between A^* and reach characteristics

The relations between A^* and the non-dimensional BTC tail (longer tail leads to larger A^* values) and between A^* and non-dimensional first arrival time (earlier arrival time leads to larger A^* values) can be attributed to the mixing and transport characteristics of the stream reach. The three physical processes that affect the BTC shape are advection, dispersion, and the amount of transient storage in the stream reach. A stream dominated by advection with minimal dispersion and transient storage would cause the tracer to quickly flush out of the measurement reach, resulting in a short duration BTC and a short BTC tail. A short BTC tail compared to a long BTC tail would correspond to a relatively smaller harmonic mean travel time (t_h), and the transformation by t_h will "collapse" the nondimensional BTC less, resulting in a later τ_0. Conversely, a stream with significant transient storage would result in a long duration BTC and a long BTC tail. A long BTC tail would correspond to a larger t_h, and the nondimensional BTC will be more collapsed, resulting in an earlier τ_0. A long tail will remain long after transformation, leading to more area under the nondimensional BTC (A^*)

when compared to a short-tailed BTC.

The high A^* values for Carnation Creek Trib L were due to the long tail of the BTCs for this stream, indicating a large amount of transient storage and/or dispersion throughout the measurement reach. Most tracer pulses from other streams were around 10 minutes long, while the pulses at Trib L lasted 20 minutes. The transient storage at Trib L was visible at the field site, as the reach contained multiple pools connected by small trickles of water, with a high bed roughness relative to the size of the wetted channel. The mean water velocity ($\bar{v}$ = 0.07 m/s) and discharge (Q = 0.009 m^3/s) measured at Trib L were lower than any other stream studied. Similar velocities ($\bar{v}$ = 0.10 to 0.23 m/s) and discharges (Q = 0.010 m^3/s to 0.040 m^3/s) were also measured at Carnation Creek Trib C for a series of injections during a rain event. For four injections, a decrease in A^* occurred in relation to an increase in discharge. The active stream channel visibly changed from many pools connected by small trickles of water at low flow, to a faster-flowing, uniform flow of water at higher flows. From these observations of the two Carnation Creek watershed streams, A^* seems highly dependent on the amount of transient storage in a stream reach. A longer tracer pulse coinciding with a stream with more transient storage will result in a higher A^* compared to a shorter tracer pulse.

Presumably, transient storage will change with discharge depending on the stream. In some streams, a higher discharge will cause areas of storage to connect with the main stream flow, resulting in less transient storage and a lower A^*. In other streams, a higher discharge will activate new areas of the channel that will pool with water, resulting in more transient storage and a lower A^*. Pemberton Creek was the only stream studied with a large range of discharges measured for a constant reach length (Figure 3.10). The lack of relation between A^* and discharge suggests that the impact of transient storage stayed constant at this stream.

As shown in Figures 3.9 and 3.11, A^* tends to decrease as the reach length is extended. This relation is most apparent when looking at the long reach length experiments at Pemberton Creek. For these three measurements, the peak EC_T at the downstream location was half the value at the upstream location, and t_h at the downstream location was four times the value at the upstream location, resulting in the value of A^* at the downstream location equal to half the value at the

upstream location. Since the peak EC_T and t_h do not scale proportionally as the measurement location is moved downstream, A^* will vary with reach length.

Measurement location can have a large effect on A^*. For example, A^* values from Mosquito Creek ranged from 0.32 to 0.46, even though all five probes were within 8 m of each other (for a measurement reach of 140 m). For a narrow stream (e.g. Trib L), measurement location seems to have less of an effect on A^* variability.

The limited metadata associated with the NHC data set (e.g. no visual observation, no reach width or slope information, no confirmation of adequate mixing length, unknown accuracy of data) makes it difficult to integrate these results into the discussion of the field study experiments. However, certain observations can be discussed. Despite the uncertainties regarding the NHC dataset, the distribution of A^* values is comparable to the field study. There were measurements at markedly higher flow levels (Q = 20, 34 and 40 m^3/s), and the resulting A^* values (0.41, 0.47, 0.58, 0.48, 0.53) were close to the average A^* value (0.55), suggesting that typical values of A^* remain similar at higher discharges.

One NHC stream at very low flow (Q = 0.003 m^3/s) had high A^* values (0.69-0.84), similar to the low flow measurements at Carnation Creek Trib L and Trib C. The tracer pulse was also very long, indicating a large amount of transient storage. In contrast, some of the other NHC data with the largest A^* values (0.92, 0.89) had short tracer pulses (5-15 minutes). This may be due to a short mixing length (possibly even too short for adequate mixing), as we have seen that A^* and reach length are inversely related.

4.4.2 Using A^* for dosage guidelines

The variability of A^* has been explored using BTCs from 21 streams (8 field study streams and 13 streams in the NHC dataset). The average A^* value (0.55) can be used as a first-order approximation to estimate the amount of salt to inject into a stream using Equation 2.14. The remaining variables in the equation are either estimated or calculated (A_c, CF_T, and L) or specified by the practitioner (the desired peak EC_T over background EC_T). Figure 4.2 and Table 4.2 show the process for determining

A^* for an example BTC from a discharge measurement. Table 4.3 shows an example salt dosage calculation.

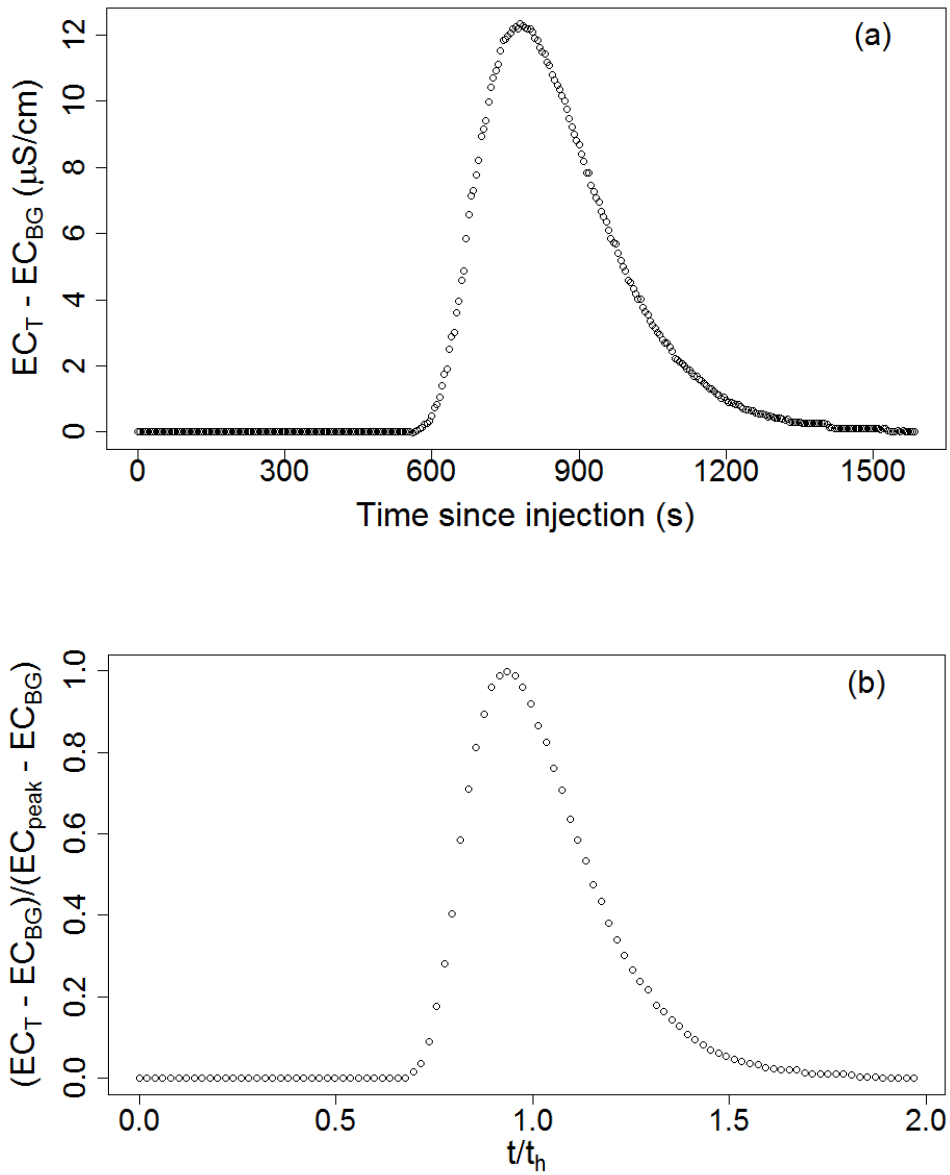

Figure 4.2: Example BTC transformation to determine A^*: (a) Original BTC, (b) non-dimensional BTC transformed by $(EC_{peak} - EC_{BG})$ and t_h. The value of A^* is the area under the curve in (b). In this example, $(EC_{peak} - EC_{BG})$ = 12.3 µS $\cdot$ cm^{-1}, and t_h = 839 s.

Table 4.2: Values for determining A^* from example BTC in Figure 4.2

Term	Description	Value
A	Area under BTC ($\mu S \cdot s \cdot cm^{-1}$)	3860
$EC_{peak} - EC_{BG}$	($\mu S \cdot cm^{-1}$)	12.3
t_h	Harmonic mean travel time (s)	836
A^*	Area under non-dimensional BTC (dimensionless)	0.38

Table 4.3: Example salt dosage calculation using A^*

Desired EC_{peak} - EC_{BG} ($\mu S \cdot cm^{-1}$)	30
Mean channel width (m)	10.0
Mean water depth (m)	1.0
Reach length (m)	200
CF_T ($g \cdot cm \cdot \mu S^{-1} \cdot m^{-3}$)	0.48
A^* (dimensionless)	0.55
Salt dosage for injection (kg)	15.8

The uncertainty of the salt dose will be based on the uncertainty of A^*, which may be taken as two times the standard deviation of all computed A^* values (0.13). The uncertainty of A^* ($\pm$ 0.26) is approximately half (50%) the mean value of A^* (0.55). The A^* uncertainty suggests that the estimate of the salt dose may be incorrect by up to 50% for a 95% confidence level. If the stream is underdosed by 50%, then the peak EC_T over background EC_T will be half of the desired value. For example, if the resulting peak EC_T over background EC_T is 15 μS/cm instead of 30 μS/cm, the discharge may still be computed, but with a higher uncertainty. If the stream is overdosed by 50%, the peak EC_T over background EC_T will be 150% of the desired value, which will only improve (decrease) the uncertainty associated with the computed discharge. Also, compared to the wide range of dosage guidelines suggested by others in Table 1.1, a 50% uncertainty in dose is reasonable. However, the dose uncertainty will increase based on the uncertainty in estimating other parameters in Equation 2.14, such as the mean depth and wetted width.

For practitioners, the ease of calculating A^* leads to the ability to generate a database of A^* values for different field sites. This database can be used to better estimate the amount of salt

needed for injection, which is especially useful for (a) measuring discharge at flow levels previously unmeasured, and (b) measuring discharge at new streams or stream reaches. A value of A^* can be more accurately estimated if previous injection data from that stream can be used, as A^* has lower in-stream variability compared to between-stream variability. The results of this study promote the following best practices to minimize A^* variability between streams and for a single stream: (1) The minimum adequate reach length should be used, as A^* has been shown to decrease with reach length; (2) Similar measurement locations should be used for different injections (e.g. always measure in fast-flowing, non-turbulent water), as A^* can vary significantly based on measurement location.

4.5 Rhodamine WT dilution gauging

4.5.1 Laboratory calibrations and experiment for Rhodamine WT

The significant difference in CF_R values for both probes between turbidity levels indicates that the amount of suspended sediment in the water affects the RWT measurement (10% and 13% difference for each probe). These differences are much higher than observed in salt calibrations, as discussed in Section 4.1.1. This effect was also observed during the lab experiment, when adding silt at approximately 16:13 resulted in a small but noticeable increase in measured fluorescence (Figure 3.12). These observations agree with Smart's and Laidlaw's (1977) results that the presence of suspended sediment raises apparent fluorescence.

Because CF_R apparently varies across streams and probes, it is necessary to perform a calibration for each gauging. Future work should explore any relationships between Rhodamine CF_R value and stream water turbidity and/or water chemistry (similar to the salt CF_T value analysis in this thesis). These relationships may provide a basis for estimating the Rhodamine CF_R factor in cases where it is not feasible to complete the calibration in the field (e.g., due to time constraints or equipment failure).

As shown in Figure 3.12, there was a continuous decline in RWT concentration over time, even with no suspended sediment present. The decay is likely due to RWT degradation from the light emitted from the measurement probe, as noted by others (Gooseff, pers. comm.). This photolytic

decay would not be an issue in the field, as the RWT would not be recirculated through the measurement probe.

There was no discernible relationship between suspended sediment concentration and rate of RWT decay (Figure 3.13). Surprisingly, the decay rate decreased with the addition of silt. The silt may effectively shield the RWT from photolytic decay during measurements. The decay of RWT due to light emission from the measurement probe and the silt additions confound any conclusions that may be made from this experiment about the effect of silt on RWT decay rates.

The "no silt content" and "low silt content" segments of the experiment had suspended sediment concentrations well below 1000 mg/L (approximately 0 mg/L and 200 mg/L, respectively). The "high silt content" segment of the experiment had a suspended sediment concentration of approximately 1200 mg/L. Smart and Laidlaw (1977) found that sorption can be an issue at sediment concentrations above 1000 mg/L or if the sediment is extremely fine or contains significant organic matter. However, in this study, there was no notable increase in RWT decay when the suspended sediment concentration exceeded 1000 mg/L.

Since the signal becomes less stable, or noisier, with higher suspended sediment concentrations, highly turbid waters may warrant a higher dosage of RWT for injection, to obtain an adequate signal:noise ratio in the discharge measurement. Also, a noisier signal could make it difficult to obtain a strong linear relation between measurement reading (in mV) and concentration during the calibration procedure. The instability of the measurement signal affected the laboratory calibrations as one can see with the high coefficients of variation in Table 3.9, which were an order of magnitude higher than the coefficients of variation from the salt calibrations (Table 3.1). A five-point (or more) calibration procedure should always be used to minimize any effects of signal instability.

4.5.2 Stream gauging with Rhodamine WT

The discharges yielded by WSC_A and $Hoskin_B$ probes agreed well with those computed from salt dilution for all injections. The downstream probes yielded a small increase in discharge compared to the upstream probes, likely due to minor tracer loss into the streambed (for both salt and Rhodamine

WT) or due to diffuse discharge of groundwater into the stream channel. This similar behavior in tracer loss between both salt and RWT indicates that RWT loss due to sorption or photolysis was likely not a factor in these measurements. If decay was an issue, an increase in discharge from the Rhodamine measurements relative to the salt measurements would have occurred for the downstream probes. If there was an active degradation process, it may be hidden in the large uncertainties for the RWT measurements.

The RWT measurement uncertainties (13.5%-43.0%) were markedly and consistently higher than the salt measurement uncertainties (3.1%-9.0%) for all measurements, due to the instability of the RWT measurement signal and large uncertainty associated with the CF_R values. The measurement discrepancies from Hoskin_A compared to Hoskin_B, WSC_A, and the conductivity probes may be attributed to the inability to conduct a confident, consistent calibration (Table 3.11). Both Hoskin probes had similar background uncertainty and peak/background ratios; the only difference was the CF_R values. The source of measurement error is unknown for WSC_B.

Duerk (1983) did not detect RWT loss in constant-rate injections in a concrete storm sewer and a concrete-lined open channel. However, sorption onto the streambed is more likely an issue for natural stream channels (versus concrete channels) due to the water and RWT filtering in and out of the streambed. Regardless, sorption with the stream bed was not apparent at the injections at Mosquito Creek for this study.

Bencala et al. (1983) and Dierberg and DeBusk (2005) measured decay due to gravel bed interactions, suspended sediment adsorption, and photolysis, but their experiments were on the time scale of hours to days, much longer than a typical slug injection measurement. The results from this study at Mosquito Creek suggest that RWT degradation may be insignificant for low turbidity streams for the duration of a typical slug injection measurement (i.e. under an hour).

Additional measurements should be performed in high turbidity streams, where sorption may be a larger concern. Many streams and rivers in B.C. have high turbidity from glacial meltwater, so a greater understanding of when Rhodamine is a viable measurement technique is invaluable, especially considering previous studies have identified significant decay processes at longer timescales

and at high suspended sediment concentrations. Smart and Laidlaw (1977) observed that dye losses due to sorption are independent of dye concentration. Therefore, if sorption is a concern, a higher dosage would minimize the relative loss of RWT for a discharge measurement.

The relatively high CF_R uncertainty (compared to salt CF_T uncertainty) and the relation between CF_R and turbidity level raise concerns for using RWT for automatic gauging setups. In automatic gauging setups, the CF_R would not be determined for each injection, and would have to be estimated. Turbidity levels will vary based on flow level, especially during storm events when the turbidity will be much higher than normal levels. Therefore, using one CF_R value for different flow levels would be inaccurate. This CF_R variability is in contrast to salt CF_T variability, where we have seen that CF_T remains relatively constant over a large range of background EC_T values.

Chapter 5

Conclusions

The first section of this chapter summarizes the important findings of this study in relation to the research objectives outlined in Section 1.3. The first section also integrates these results with suggestions for best practices. The final section discusses areas where further study would be beneficial for improving tracer dilution stream gauging.

5.1 Summary of key results

Calibration procedure of salt tracer dilution. The first four experiments revealed the following. There were minor ($< 1\%$) and statistically insignificant differences in the precisions associated with the following variations in calibration procedure: (1) the use of glass pipettes versus autopipettes, (2) mixing a new secondary solution for each calibration versus using the same secondary solution for each calibration, and (3) using distilled water in the secondary solution (with the appropriate distilled water correction) versus using stream water in the secondary solution. Therefore, the choice of methodology for these different calibration approaches should be based on user preference. Despite the temperature compensation applied by the probes, calibrating at air temperature in the laboratory yielded significantly different values of CF_T from calibrating at the stream temperature. Therefore, calibration should be performed at in-situ temperature whenever possible.

For the water sample CF_T analysis from samples from British Columbia and Yukon, a significant

positive linear relation between CF_T and EC_{BG} was found for the water samples with $EC_{BG} < 600$ $\mu S \cdot cm^{-1}$. The water samples with $EC_{BG} > 1000$ $\mu S \cdot cm^{-1}$ did not follow this trend, likely due to differences in the relative concentrations of various cations and anions. The high EC_{BG} water samples imply that (a) a confident estimation of CF_T based on a linear relation with EC_{BG} may not be possible for water samples with high EC_{BG}, and/or (b) regional relations between CF_T and EC_{BG} may be more applicable (e.g. separate relations for British Columbia and Yukon) versus a universal relation.

Also, it was found that different probes can behave differently when calibrating the same stream water, and therefore the discharge measurement and calibration procedure should always be performed with the same probe. Table 4.1 can guide users when determining the uncertainty associated with the CF_T value.

Mixing lengths. The minimum adequate mixing length was found to lie between 6.5 and 24.5 wetted widths for the study reaches, in general agreement with Day's (1977) recommendation of 25 wetted widths. Mixing length was reach dependent. Placing probes on opposite sides of the stream is required to verify with confidence that adequate mixing has occurred, as probes on the same side of the stream may yield similar discharges even if the tracer is not well mixed across the stream channel. If placement on both sides of the stream is not possible, then the measurement reach length should be at least 25 wetted widths downstream of the injection point to ensure the tracer is fully mixed across the stream channel at the measurement location. In channels without good lateral mixing (e.g. shallow gradient channels), using an adequate mixing length may not be feasible or possible. However, in these cases, the velocity-area method will likely be the more appropriate discharge measurement method.

Surface and subsurface discharge into the channel can confound the determination of x_m and result in ambiguous discharge measurements, as seen in this study and reported by others (Zellweger et al., 1989; Clow and Fleming, 2008). Therefore, the shortest possible mixing reach should be used when possible to minimize effects of lateral water inputs. Lateral water fluxes will likely be a larger issue for smaller streams since they will have a larger relative impact on the total flow. One could

take point measurements of EC_T along the stream reach to help diagnose the existence of significant lateral inputs, since varying values of EC_T suggests inflow from a different water source (Moore et al., 2008).

Discharge measurement variability due to measurement location. The choice in measurement location can significantly affect the discharge measurement, even downstream of adequate mixing. Differences in derived discharge were as high as 9% between different probe locations for the same measurement. Generally, it is best to be consistent in measurement location (e.g. always place probes in areas of fast-moving water). Aerated areas and side pools tend to produce choppy BTCs, indicating that the tracer is arriving in clumps (i.e. not adequately mixed). Probes in fast-moving chutes of water resulted in the smoothest BTCs, which suggests (but does not confirm) that the tracer is well-mixed across the channel. Therefore, it is advised to place probes in fast-moving (non-aerated) water when possible. The practitioner should provide detailed descriptions and/or photographs of the measurement locations to assist in documenting factors that influence the accuracy of a measurement.

Dosage guidelines. Using Equation 2.14, the dosage can be estimated based on estimates of channel geometry, desired peak tracer concentration over background tracer concentration, and the nondimensional area under the BTC, A^*. Analyzing 165 BTCs, a first-order estimate of A^* was found to be equal to 0.55, with a standard deviation equal to 0.13. Using two times the standard deviation as a measure of A^* uncertainty, the uncertainty is approximately $\pm$ 50%, suggesting that using this dosage approach may underdose or overdose the stream by up to 50%.

The variability of A^* decreased when focusing on a specific stream reach. The value of A^* also seems to be dependent on reach length, the amount of in-stream storage in the stream reach, and measurement location. Therefore, a more accurate estimate of A^* can be used, based on previous injections from a stream reach.

The practitioner can generate a database of A^* values, with detailed descriptions of measurement location, measurement reach length, and other experiment conditions. He/She can use this database to choose a value of A^* to use to determine injection dosage. For example, if a practitioner is

continuously returning to a stream reach for discharge measurements, he/she may use an A^* value specific to that stream reach. As this database is populated, between-stream trends may become apparent, such as a relation between A^* and channel morphology, which can assist the practitioner in choosing an A^* value for measuring discharge at new field sites.

Rhodamine WT dilution gauging. The CF_R value from Rhodamine WT calibrations varied significantly as a function of the water's turbidity level, indicating that calibration is required for each discharge measurement (moreso than salt CF_T determination). Also, the variability of repeated calibrations for RWT was an order of magnitude higher than for salt. It is recommended that at least five points be used in the calibration procedure to minimize problems associated with instability of the measurement signal. Due to these uncertainties associated with the calibration procedure, automatic gauging with RWT (using an estimated CF_R value) may not be accurate. The laboratory and field experiments focused on RWT decay due to sorption and photolysis were confounded by other factors, and no conclusions can be made on the effect of decay on the measurement. Regardless of decay, measurement uncertainties were consistently and markedly higher for the RWT probes (13.5%-43.0%) than for the salt probes (3.1%-9.0%) for the field measurements.

5.2 Future research

This study has explored many aspects of tracer dilution stream gauging and the potential uncertainties involved. Future research should focus on a full integration of all aspects of this streamflow measurement technique into a standard operating procedure (SOP). This SOP should document a range of practices with associated uncertainties to allow flexibility under varying field conditions. An SOP will prove to be an invaluable asset to practitioners and scientists as we strive to quantify and minimize measurement uncertainty.

For the salt calibration procedure, additional work should be done with high EC_{BG} (greater than 1000 $\mu S \cdot cm^{-1}$) water samples. It will be useful to know how well the distilled water correction works when using distilled water in the secondary solution for these high EC_{BG} samples. Also, additional data in this range will help us understand the relation between CF_T and EC_{BG}, and which

specific ions may have the greatest effect on CF_T variability. Lastly, more controlled, concurrent calibrations with different brands of conductivity probes are warranted to better understand the variability between measurement devices. Sentlinger and Zimmermann (pers. comm.) have already done significant work in CF_T uncertainty, independent of the work presented in this thesis and in collaboration with the author of this thesis.

A more detailed study focusing specifically on mixing lengths may reveal stronger relations between reach morphology and adequate mixing lengths. These relations can be valuable, as this study has shown the presence of measurement error arising from mixing length ambiguity. A better estimate of minimum adequate mixing length will help minimize effects of lateral water fluxes.

To improve upon the dosage guidelines introduced in this study, a first step would be for users to test the guidelines in the field. The user can estimate dosage based on estimates of A^*, reach geometry, and a desired peak EC_T over background EC_T, and observe how close the actual peak EC_T over background EC_T is to the target value. Further exploration of non-dimensional BTCs and their associated non-dimensional area under the curve of the BTCs (A^*) can refine and build upon the dosage guidelines. Specifically, the variability of A^* in relation to stream morphology and flow level (within stream and between streams) will guide higher accuracy dosage guidelines. The ecological impact of stream tracers is a major concern for this technique, and a consistent, standard dosage guideline can help ensure that toxicity threshholds are not exceeded.

This study attempted to quantify Rhodamine WT decay due to sorption and photolysis. Previous studies (e.g. Smart and Laidlaw, 1977; Duerk, 1983; Dierberg and DeBusk, 2005) reported various levels of RWT decay, but many of the results were limited to laboratory experiments or during field experiments over long time periods (significantly longer than a dilution gauging tracer pulse). Future research on RWT should focus on the effect of water chemistry and/or turbidity on the calibration factor (similar to the salt calibration study described in this thesis), and on field experiments on high turbidty streams.

References

Bencala, K. E., Rathbun, R. E., Jackman, A. P., Kennedy, V. C., Zellweger, G. W., and Avanzino, R. J. 1983. Rhodamine WT dye losses in a mountain stream environment. *Journal of the American Water Resources Association*, 19(6):943–950.

Clow, D. W. and Fleming, A. C. 2008. Tracer gauge: An automated dye dilution gauging system for ice-affected streams. *Water Resources Research*, 44(12). W12441.

Comiti, F., Mao, L., Wilcox, A., Wohl, E. E., and Lenzi, M. A. 2007. Field-derived relationships for flow velocity and resistance in high-gradient streams. *Journal of Hydrology*, 340(12):48 – 62.

Day, T. J. 1977. Observed mixing lengths in mountain streams. *Journal of Hydrology*, 35(1):125–136.

Dierberg, F. E. and DeBusk, T. A. 2005. An evaluation of two tracers in surface-flow wetlands: Rhodamine-WT and lithium. *Wetlands*, 25(1):8–25.

Duerk, M. D. 1983. Automatic dilution gaging of rapidly varying flow. Water Resources Investigations Report 83-4088, United States Geological Survey, Washington, DC, U.S.A.

Fischer, H. B. 1966. Longitudinal dispersion in laboratory and natural channels. Technical Report KH-R-12, California Institute of Technology.

Glover, R. 1964. Dispersion of dissolved or suspended materials in flowing streams. Professional Paper 433B, United States Geological Survey, Washington, DC, U.S.A.

Gomi, T., Sidle, R. C., and Richardson, J. S. 2002. Understanding processes and downstream linkages of headwater systems. *BioScience*, 52(10):905–916.

Gonalez-Pinzon, R., Haggerty, R., and Dentz, M. 2013. Scaling and predicting solute transport processes in streams. *Water Resources Research*, 49(7):4071–4088.

Hem, J. 1982. Conductance: a collective measure of dissolved ions. In Minear, R. and Keith, L., editors, *Water Analysis: Vol. 1. Inorganic Species*, pages 137–161. Academic Press, New York.

Herschy, R. 1975. *The Accuracy of Existing and New Methods of River Gauging*. University of Reading, Reading, UK.

Hudson, R. and Fraser, J. 2002. Alternative methods of flow rating in small coastal streams. Forest research extension note EN-014, British Columbia Forest Service, Vancouver Forest Region, Nanaimo, BC.

Hudson, R. and Fraser, J. 2005. Introduction to salt dilution gauging for streamflow measurement part 4: The mass balance (or dry injection) method. *Streamline Watershed Management Bulletin*, 9(1):6–12.

Jimnez, M. A. and Wohl, E. 2013. Solute transport modeling using morphological parameters of steppool reaches. *Water Resources Research*, 49(3):1345–1359.

Kelleher, C., Wagener, T., McGlynn, B., Ward, A. S., Gooseff, M. N., and Payn, R. A. 2013. Identifiability of transient storage model parameters along a mountain stream. *Water Resources Research*, 49(9):5290–5306.

Kilpatrick, F. A. 1970. Dosage requirements for slug injections of Rhodamine BA and WT dyes. Professional Paper 700-B, United States Geological Survey, Washington, D.C., U.S.A.

Kilpatrick, F. A. and Cobb, E. D. 1985. Measurement of discharge using tracers. Techniques of Water-Resources Investigations A16, United States Geological Survey, Washington, DC, U.S.A.

Kite, G. 1993. Computerized streamflow measurement using slug injection. *Hydrological Processes*, 7(2):227–233.

Lee, A. J. and Ferguson, R. I. 2002. Velocity and flow resistance in step-pool streams. *Geomorphology*, 46(1):59–71.

Letvak, D., Richards, R., and staff, R. I. B. 1998. Manual of standard operating procedures for hydrometric surveys in british columbia. Manual 1.0, Ministry of Environment, lands and Parks, Victoria, BC.

Liu, Y., Freer, J., Beven, K., and Matgen, P. 2009. Towards a limits of acceptability approach to the calibration of hydrological models: Extending observation error. *Journal of Hydrology*, 367(12):93–103.

McMillan, H., Krueger, T., and Freer, J. 2012. Benchmarking observational uncertainties for hydrology: rainfall, river discharge and water quality. *Hydrological Processes*, 26(26):4078–4111.

Moore, R. D. 2003. Introduction to salt dilution gauging for streamflow measurement: part 1. *Streamline Watershed Management Bulletin*, 7(4):20–23.

Moore, R. D. 2005. Introduction to salt dilution gauging for streamflow measurement part 3: slug injection using salt in solution. *Streamline Watershed Management Bulletin*, 8(2):1–6.

Moore, R. D., Richards, G., and Story, A. 2008. Electrical conductivity as an indicator of water chemistry and hydrologic process. *Streamline Watershed Management Bulletin*, 11(2):1–6.

Oberg, K. and Mueller, D. S. 2007. Validation of streamflow measurements made with acoustic doppler current profilers. *Journal of Hydraulic Engineering*, 133(12):1421–1432.

Pelletier, P. M. 1988. Uncertainties in the single determination of river discharge: a literature review. *Canadian Journal of Civil Engineering*, 15(5):834–850.

R Core Team, R. 2015. *R: A Language and Environment for Statistical Computing*. R Foundation for Statistical Computing, Vienna, Austria.

Smart, P. L. and Laidlaw, I. M. S. 1977. An evaluation of some fluorescent dyes for water tracing. *Water Resources Research*, 13(1):15–33.

Szeftel, P., Moore, R. D., and Weiler, M. 2011. Influence of distributed flow losses and gains on the estimation of transient storage parameters from stream tracer experiments. *Journal of Hydrology*, 396(3):277–291.

Turnipseed, D. P. and Sauer, V. B. 2010. Discharge measurements at gauging stations. Techniques and Methods 3-A8, United States Department of the Interior and United States Geological Survey, Washington, D.C., U.S.A.

Ward, A. S., Gooseff, M. N., Voltz, T. J., Fitzgerald, M., Singha, K., and Zarnetske, J. P. 2013. How does rapidly changing discharge during storm events affect transient storage and channel water balance in a headwater mountain stream? *Water Resources Research*, 49(9):5473–5486.

Ward, P. R. B. 1973. Prediction of mixing lengths for river flow gaging. *ASCE Journal of the Hydraulics Division*, 99(7):1069–1081.

Westerberg, I., Guerrero, J., Seibert, J., Beven, K. J., and Halldin, S. 2011. Stage-discharge uncertainty derived with a non-stationary rating curve in the Choluteca River, Honduras. *Hydrological Processes*, 25(4):603–613.

Wood, P. and Dykes, A. 2002. The use of salt dilution gauging techniques: ecological considerations and insights. *Water Research*, 36(12):3054 – 3062.

Yotsukura, N. and Cobb, E. D. 1972. Tranverse diffusion of solutes in natural streams. Professional Paper 582-C, United States Geological Survey, Washington, D.C., U.S.A.

Zellweger, G. W., Avanzino, R. J., and Bencala, K. E. 1989. Comparison of tracier-dilution and current-meter discharge measurements in a small gravel-bed stream, little lost man creek, californation. Water-Resources Investigations Report 89-4150, United States Geological Survey, Menlo Park, CA, U.S.A.